ISSN: 2683-2658

RENEWABLE ENERGY, BIOMASS & SUSTAINABILITY

NOVEMBER 2026 Vol. 8, No. 2

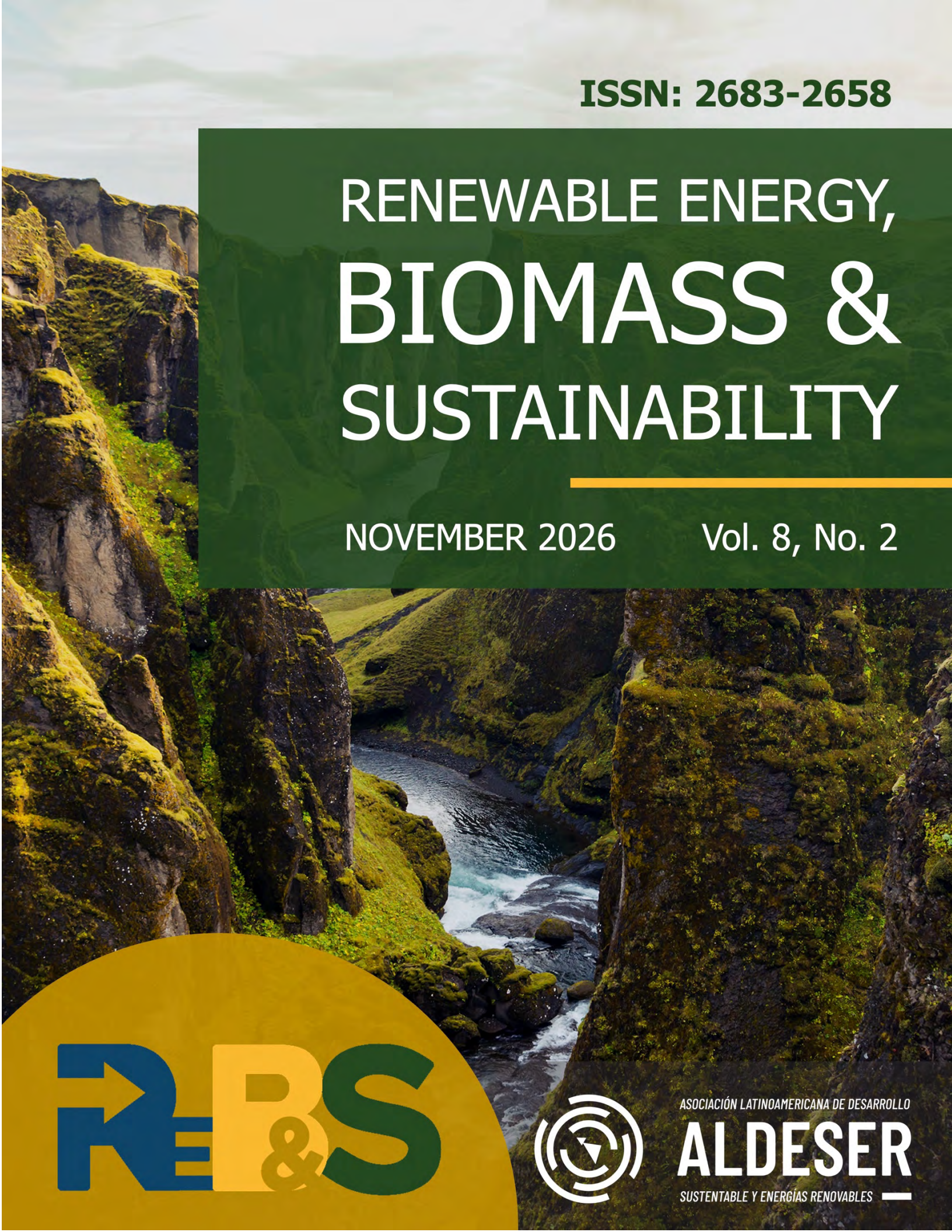

RE&S

ASOCIACIÓN LATINOAMERICANA DE DESARROLLO
ALDESER
SUSTENTABLE Y ENERGÍAS RENOVABLES

Renewable Energy, Biomass & Sustainability
Vol. 8 No. 2 (2026)

Published: April 25, 2026

Renewable Energy, Biomass & Sustainability, Vol. 8, No. 2, November 2026, is a biannual publication, published and edited by Asociación Latinoamericana de Desarrollo Sustentable y Energías Renovables A.C. (ALDESER), Sur 4 No. 270, Colonia Centro, C.P. 94300, Orizaba, Veracruz, Mexico, Tel. 2722372285, Web Page: https://aldeser.org/revistas.html and email address: secretariat@aldeser.org.

The Reservation of Rights of Exclusive Use Certificate No.: 04-2025-060617423800-102, ISSN: 2683-2658, are both granted by the Instituto Nacional del Derecho de Autor (INDAUTOR, Mexico). Responsible for the last update of this issue: Andrea Alvarado Vallejo. Date of last modification, April 25, 2026.

Table of Contents

Conceptual Prototype of Blue and Green Infrastructure for Domestic Stormwater Management in Semi-Arid Zones

Dina Margarita Olmedo-Martínez [1], Carlos Alfredo Bigurra-Alzati [2], Liliana Lizárraga Mendiola [2], Omar Salvador Areu-Rangel [2], Marcelino Antonio Zúñiga-Estrada [3], Claudia Coronel-Olivares [1] y Gabriela A. Vázquez-Rodríguez [1,*]

[1] Chemistry Department, Universidad Autónoma del Estado de Hidalgo (UAEH), Mineral de la Reforma, Hidalgo, México
[2] Engineering and Architecture Department, UAEH, Mexico
[3] Earth and Materials Sciences Department, UAEH, Mexico
* Corresponding author: gvazquez@uaeh.edu.mx

Received: June 14, 2025 Accepted: July 26, 2025 Published: April 26, 2026
DOI: https://doi.org/10.56845/rebs.v8i2.669

Abstract: This paper presents the conceptual design of a blue and green infrastructure (BGI) prototype focused on decentralized stormwater collection, treatment, and storage in urban dwellings located in semi-arid regions. The proposal is presented as an adaptation strategy to address water scarcity, considering the limited performance of conventional water supply systems in such vulnerable contexts. The BGI system integrates two complementary strategies: direct collection from rooftops and the collection of surface runoff generated on impervious sidewalks, which is conveyed through permeable pavement to a bioretention cell composed of vegetation and recycled construction aggregates. This configuration allows runoff water to be collected, filtered, and stored for later use. Local climate data were used to estimate surface runoff, infiltration within the system layers, and potential storage through a preliminary water balance. The design was applied to a typical home with a roof area of 39.2 m^2 and a daily consumption of 724.9 liters (for five inhabitants, using water-saving devices). The results indicate that, during representative rainfall events, the volume captured partially covers this allocation for at least one day, demonstrating the hydraulic viability of the system in urban environments with limited space. It should be noted that the water balance does not account for losses due to evaporation or evapotranspiration, as the objective was to provide a preliminary estimate for conceptual sizing. It is concluded that the BGI prototype represents a viable and sustainable alternative for rainwater harvesting in homes with limited space and restricted access to conventional water sources, thus contributing to a circular water economy.

Keywords: nature-based solutions, rainwater harvesting, decentralized water management

Introduction

Secure, continuous access to water is one of the main challenges facing large regions of the world, especially countries of the Global South, such as Mexico. It is estimated that more than 10 million people in the country lack reliable access to drinking water (Lluch-Cota, 2022), a situation that is exacerbated in arid and semi-arid regions, where low rainfall and limited infrastructure increase water vulnerability among the population (Carril-Ferreira *et al.,* 2024). This problem is further intensified by unplanned urban growth, which has led to an increase in impervious surfaces and, with it, reduced rainwater infiltration, increased surface runoff, and decreased water availability (Gregory, 2021).

In this context, it is therefore a priority to develop decentralized solutions that enable the collection, treatment, and reuse of stormwater locally. It is essential to recognize that stormwater may originate from both direct rainfall on surfaces such as roofs and sidewalks, and from runoff generated on urban surfaces. This broader approach to water collection maximizes the use of water resources that would otherwise be lost. Blue and green infrastructure (BGI) systems, also known as nature-based solutions, contribute to this effort and have been widely promoted as sustainable strategies for urban stormwater management (Vázquez-Rodríguez *et al*., 2024). Recent research highlights their ability to reduce runoff volume, improve water quality, and promote aquifer recharge, while enhancing climate resilience (Fletcher *et al.,* 2015; Liu *et al.,* 2020; Zúñiga-Estrada *et al.,* 2024).

In particular, the integration of systems such as permeable pavements and bioretention cells has proven effective for stormwater management in densely populated urban areas (Brown *et al.,* 2015). Furthermore, these solutions align with the principles of the circular economy by encouraging the local reuse of stormwater, reducing dependence on conventional water sources, and promoting more efficient and sustainable management of resources. Within this framework, this study proposes a conceptual design for a household-scale BGI system for stormwater collection, treatment, and reuse, adapted to a low-income housing unit located in a semi-arid region of central Mexico. The BGI system integrates permeable pavement and a bioretention cell. The proposal is based on local climate analysis, the

characterization of the dwelling, the estimation of domestic water demand, and the calculation of the water balance of the BGI system. The main contribution of the study is the development of a preliminary and replicable solution for low-income housing that reduces dependence on conventional water supplies through the use of stormwater.

Materials and Methods

Study area

The study micro-watershed is located in the Colinas de Plata subdivision, in the municipality of Mineral de la Reforma, Hidalgo, Mexico, at an average altitude of 2,433 m above sea level and with an area of 1.43 km² (Figure 1). The climate is classified as temperate semi-arid, characterized by intense, short duration rainfall occurring from May to October, with annual precipitation ranging from 160 to 700 mm and an average temperature of 14 °C. The area presents an average slope of 9.5% and a predominant Phaeozem soil type with a sandy clay texture. Previous studies in the area have reported that more than 70% of annual rainfall is lost through evaporation, while urbanization has significantly increased surface runoff (Bigurra-Alzati et al., 2021). These conditions justify the selection of the study area for evaluating strategies for stormwater harvesting and reuse through BGI systems.

Prototype housing

Three types of housing were identified within the study micro-watershed: small, medium, and large, based on built area and occupancy capacity. The medium category, known as “popular housing”, was selected as the prototype housing, as it is the most representative in the area studied. This type of housing is designed to accommodate up to five residents and has a total lot area of 90 m² (Figure 2). The catchment areas for rainwater and runoff were delineated using Google Earth Pro software.

Figure 1. Aerial view of the micro-watershed study, located in Mineral de la Reforma, Hidalgo. Image obtained from Google Earth

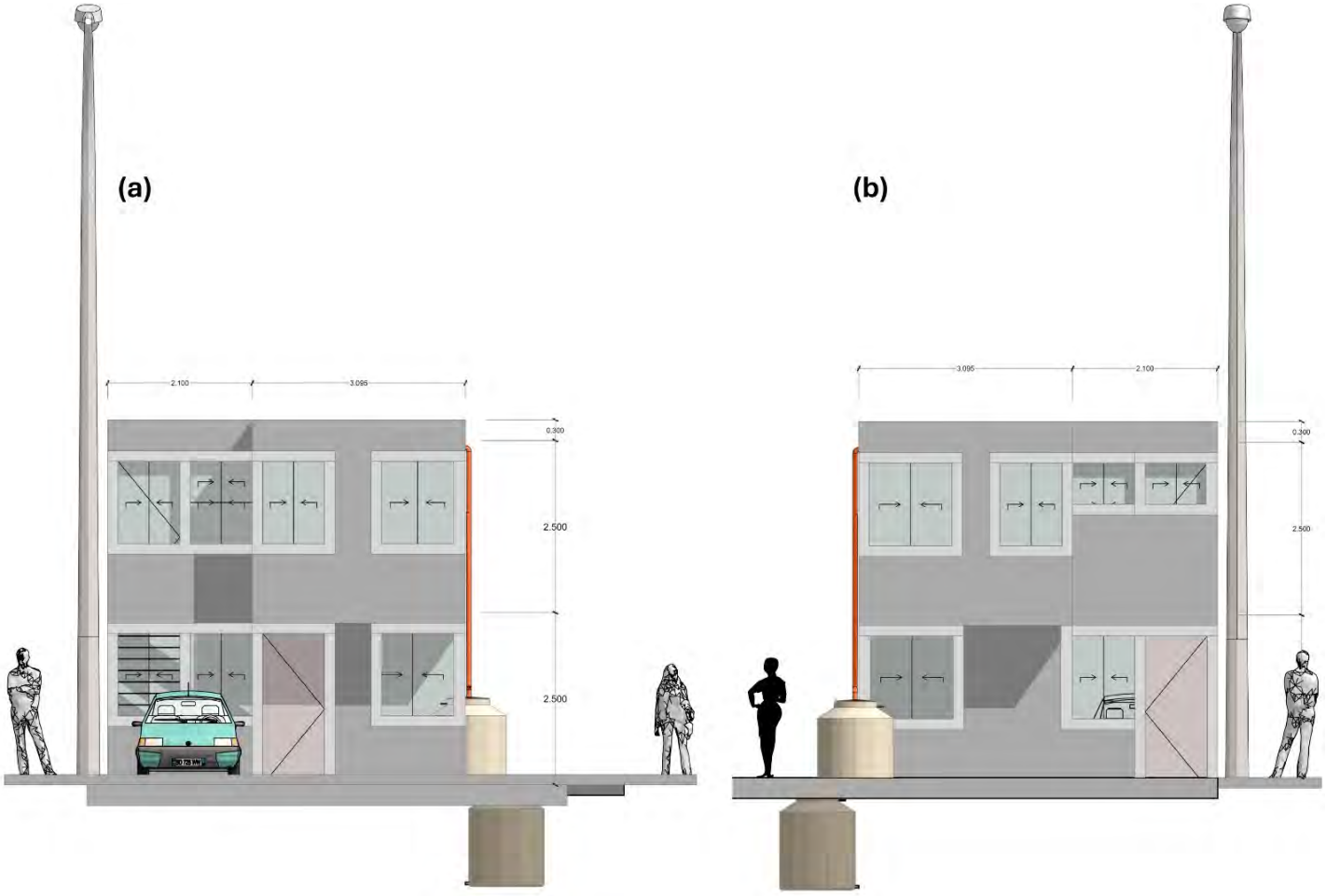

Figure 2. Architectural diagram of the prototype middle-class housing unit. (a) Main facade; (b) rear facade

Estimation of monthly rainfall volume collected

To estimate the volume of rainfall that can be collected from the prototype house's roof surface, historical climate data for the period 1981–2023 were compiled. Precipitation data were obtained from weather stations 13022 and 13056, selected for their geographic proximity and climatic representativeness relative to the study area, operated by the Comisión Nacional del Agua (CONAGUA). Based on the precipitation records, net rainfall was calculated using the methodology proposed by Anaya-Garduño (2011). This value represents the amount of water available for collection, accounting for losses due to splashing, evaporation, surface friction, and drop size. The formula used to estimate net rainfall is Equation 1:

$$PN = P * \eta \quad \textbf{(1)}$$

where $\boldsymbol{PN}$ is the net rainfall (mm), $\boldsymbol{P}$ is the mean rainfall (mm), and $\boldsymbol{\eta}$ is the rainwater capture efficiency; the value considered for this parameter was 0.765, according to Anaya-Garduño (2011).

Once the value of $\boldsymbol{PN}$ was obtained, the monthly net capture volume ($\boldsymbol{V_m}$, in m³) was calculated considering the catchment area $\boldsymbol{A}$ (m²), as shown in Equation 2. The calculation was performed monthly to identify the periods with the highest water availability.

$$V_m = \frac{PN \cdot A}{1000} \quad \textbf{(2)}$$

Estimating water demand in the prototype home

To estimate residential water demand, daily per capita water consumption was first calculated based on average consumption for various domestic activities, such as showering, using the toilet, using a washing machine, cooking, washing dishes, and cleaning the home. To do this, we used data from scientific literature and official sources. Once the individual allowance was obtained, the total monthly demand for the prototype home was estimated, assuming it is occupied by five people. This estimate was made under two scenarios: (i) assuming the use of traditional devices and (ii) considering the implementation of water-saving devices. This comparison allowed for an evaluation of the potential impact of efficient water use on total consumption. In both cases, Equation 3 proposed by Anaya-Garduño (2011) was applied to calculate the monthly demand.

$$Dj = \frac{Nu \cdot Dot \cdot Nd}{1000} \quad \textbf{(3)}$$

where $\boldsymbol{Dj}$ is the monthly water demand, expressed in cubic meters per month (m³/month); $\boldsymbol{Nu}$ is the number of beneficiaries or inhabitants of the household (persons); $\boldsymbol{Dot}$ is the daily per-capita water allocation (liters/person/day); and $\boldsymbol{Nd}$ is the number of days in the month considered.

Conceptual design of the prototype

A water balance was performed to estimate the volume of water entering the BGI system from rainfall on impervious surfaces. This analysis allowed the quantification of the inflow, infiltration, and storage flows associated with the hydraulic performance of the proposed system. For the analysis, a rainfall event lasting one hour, with an intensity of 0.045 m/h and a return period of 25 years, was selected, in accordance with the isohyets prepared by the Secretaría de Comunicaciones y Transportes (SCT) for the city of Pachuca, Hidalgo. The water balance was calculated considering three main units of the BGI system: the impervious sidewalk, the permeable pavement, and the bioretention cell. To estimate the maximum surface runoff flow, the rational method (Bigurra-Alzati *et al.,* 2021) was used, applying Equation 4.

$$Q = 0.278 \cdot Ce \cdot i \cdot A \quad \textbf{(4)}$$

where $\boldsymbol{Q}$ is the maximum runoff flow (m³/s); $\boldsymbol{Ce}$ is the runoff coefficient (dimensionless); $\boldsymbol{i}$ is the rainfall intensity (mm/hour); and $\boldsymbol{A}$ is the area considered (m²). The $\boldsymbol{Ce}$ values used were 0.9 for the impervious sidewalk, and 0.3 for the permeable pavement and the bioretention cell. To calculate the infiltrated volume, the same equation was used, substituting $\boldsymbol{Ce}$ with $\boldsymbol{1 - Ce}$.

Results and Discussion

Estimation of monthly rainfall volume collected

The average monthly precipitation values recorded between 1981 and 2023 are shown in Figure 3, indicating that most precipitation occurs from May to September, with a maximum in July (94.56 mm). In contrast, January, February, November, and December have significantly lower values, with precipitation below 40 mm. A *Ce* of 0.9 was used to calculate *PN*, based on Anaya-Garduño's (2011) findings for a concrete roof surface. Figure 4 shows the monthly values of estimated *PN* on the roof surface of the prototype house.

Figure 5 shows the monthly volume of rainwater collection, calculated from the *PN* values and the roof area (39.2 m²). The highest volumes are recorded in June, September, and July, while February, December, and January have the lowest values. This reflects the limited collection potential during the dry season, when the average monthly collection volume is 1.79 m³.

The estimated monthly catchment volumes in this study (between 0.847 and 2.84 m³) for an area of (39.2 m²) were compared with those reported by Lizárraga-Mendiola *et al.* (2015), obtained in the same geographical area on roofs of 45 m². Both studies are based on comparable annual precipitation values (552 mm in this study and 585 mm in the

cited study); however, the catchment results differ notably. This is mainly due to the methodological approach adopted in each case. While this study considers a net catchment scheme that takes into account losses due to splashing, evaporation, and structural efficiency, the study by Lizárraga-Mendiola *et al.* (2015) used the gross precipitation of the rainiest year in the period 1980–2013 (2010), allowing the identification of maximum catchment potential to be identified under an extreme scenario, without applying adjustments for losses.

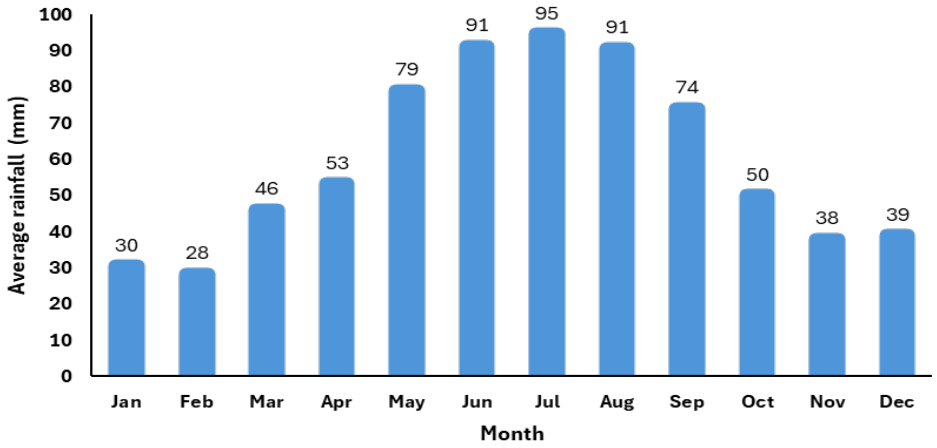

Figure 3. Average monthly precipitation recorded during the period 1981–2023

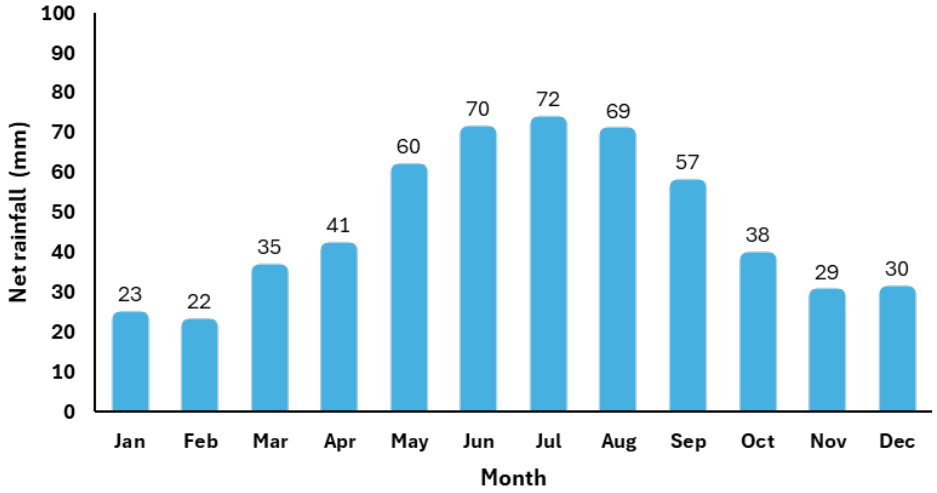

Figure 4. Net rainfall for the roof surface of the prototype house

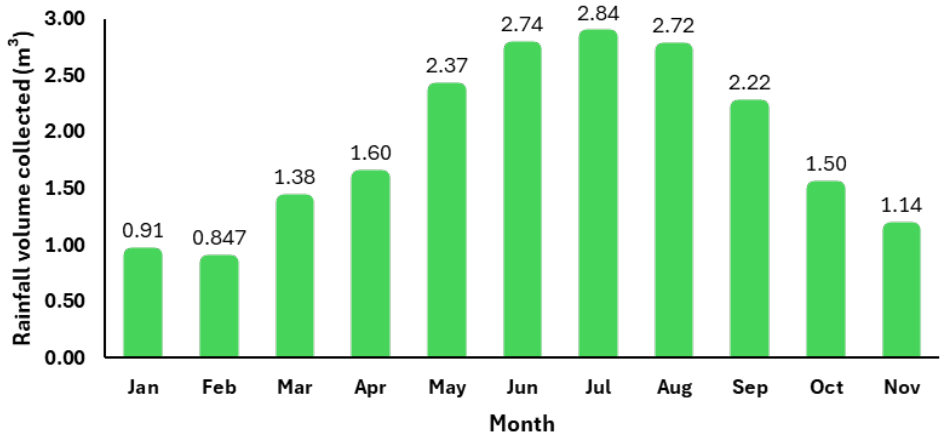

Figure 5. Rainwater collection volume on the roof of the prototype house

Estimation of water demand in the prototype dwelling

Per capita water use was estimated for two scenarios: traditional devices and water-saving devices (Table 1). A difference of 90.76 L/person/day was observed, with values decreasing from 235.74 L/person/day in the scenario with traditional devices to 144.98 L/person/day with water-saving devices, representing a 38.5% reduction. This decrease is mainly attributed to more efficient water use in showers and toilets, which together account for the highest consumption.

Table 1. Daily per capita water consumption by household activity for scenarios with traditional and water-saving devices.

Activity	Traditional (L/person/day)	Water saving (L/person/day)
Shower	109.6	62.4
WC	65.8	35.7
Dishwashing	42	30.7
Washing machine	7.71	5.6
House cleaning	1.03	1.03
Irrigation	8	8
Food preparation	1.6	1.6

The average shower duration was estimated at eight minutes per person per day (Kordana *et al.,* 2014; Kenway *et al*., 2019). Toilet use was estimated at an average of seven flushes per person per day (Lizarraga-Mendiola *et al*., 2015; Crouch *et al.,* 2021; Wilkes *et al.,* 2005). Dishwashing was estimated at three sessions per day, each lasting seven minutes, totaling 21 minutes per household per day (Shan *et al.,* 2015; Pavlou *et al.,* 2024). For washing machine use, three cycles per week were assumed, equivalent to 0.43 cycles per household per day (Beemkumar & Mathews, 2015; Pakula & Stamminger, 2009; Rosas-Flores & Morillón-Gálvez, 2010). Household cleaning was estimated at 36 liters per household per week, equivalent to 5.14 liters per day (Otsuka *et al.,* 2013; Dobroski, 2016), and watering of green areas or planters was calculated at five minutes per household per day (Willis *et al.,* 2015; Devkota *et al.,* 2015; Sandr *et al.,* 2016). Finally, the volume used for food preparation was set at eight liters per household per day (Ismail *et al.,* 2024; Makki *et al.,* 2013; Ramírez-Escobar & Buriticá-Arboleda, 2021). For activities shared by all household members, the total volume was divided by five to obtain the daily consumption per person. This approach enabled more accurate identification of the impact of efficient devices on potential water savings in the domestic sphere.

Conceptual design of the blue and green infrastructure prototype

Based on Figure 6, a prototype of the BGI system is proposed that integrates two main strategies for capturing, treating, and utilizing stormwater at the household level: direct rainwater harvesting and runoff collection from impervious surfaces.

Direct rainwater harvesting

As a complement to the BGI system, the installation of a rainwater harvesting tank is proposed to collect water from the rooftop, which has a surface area of 39.2 m^2. A downspout system will convey the collected water to the cistern (Figure 6). Preliminarily, the use of a 100-liter tank is proposed, as this capacity allows storage of the estimated daily collection during July, the rainiest month of the year, in which a total volume of 2.84 m^3 is recorded. This amount is distributed over 30.5 days, resulting in an average daily collection of approximately 93 liters. Although this amount represents only a fraction of the household's total consumption, estimated at 724.9 liters per day for a family of five with an individual allocation of 144.98 L/person/day, the continuous use of the collected water prevents the tank from reaching its maximum capacity. Thus, the resource is continuously utilized, and dependence on the municipal drinking water network is partially reduced, particularly during the months with the highest rainfall.

Surface runoff collection and treatment

The BGI system begins at the pedestrian access sidewalk, which is built with hydraulic concrete and covers an area of 7.875 m², generating surface runoff during rainfall events (Figure 6). This runoff is directed by a 2% slope toward a permeable pavement in the L-shaped pedestrian access area (13.929 m²), where infiltration begins. The permeable pavement is proposed to consist of 15 cm thickness to allow initial water infiltration; a 5 cm subbase, which distributes loads and stabilizes the system; and a 25 cm subgrade layer, which temporarily stores infiltrated water and conveys it to the next unit. Subsequently, through a controlled slope, the flow is directed to a bioretention cell, located in the lateral infiltration trench (22.301 m²). This cell has an inverted trapezoidal shape, with an upper section 90 cm wide and a lower base 30 cm wide, designed to facilitate the passage of filtered water to an underground cistern. The cell is composed, from top to bottom, of a 5 cm space at the top for managing excess water during heavy rains; 5 cm of soil, where *Chrysopogon zizanioides* (vetiver) can be planted to promote the removal of contaminants (Aguirre-Álvarez *et al.,* 2024); and 30 cm of filter material. The water that passes through this cell is finally collected in an underground storage tank located just at the end of the cell, represented in the image by white dotted lines (Figure 6). This tank stores treated water for later reuse.

In other studies, such as those by Brown *et al.* (2012), Anderson *et al.* (2013), and Tirpak *et al.* (2021), systems combining permeable pavement and bioretention cells were implemented for stormwater treatment. In all cases, favorable results were reported, including reductions in runoff volume and improvements in water quality. These systems proved effective at reducing nutrient concentrations (nitrogen and phosphorus), heavy metals concentrations (such as copper and zinc), suspended solids, and peak flows. In addition, their capacity to store and infiltrate stormwater was verified, enabling its reuse in activities that can use non-potable water. The implementation of these systems at scale in urban environments reinforces the technical viability of decentralized solutions based on BGI, similar to the conceptual design of the system proposed here.

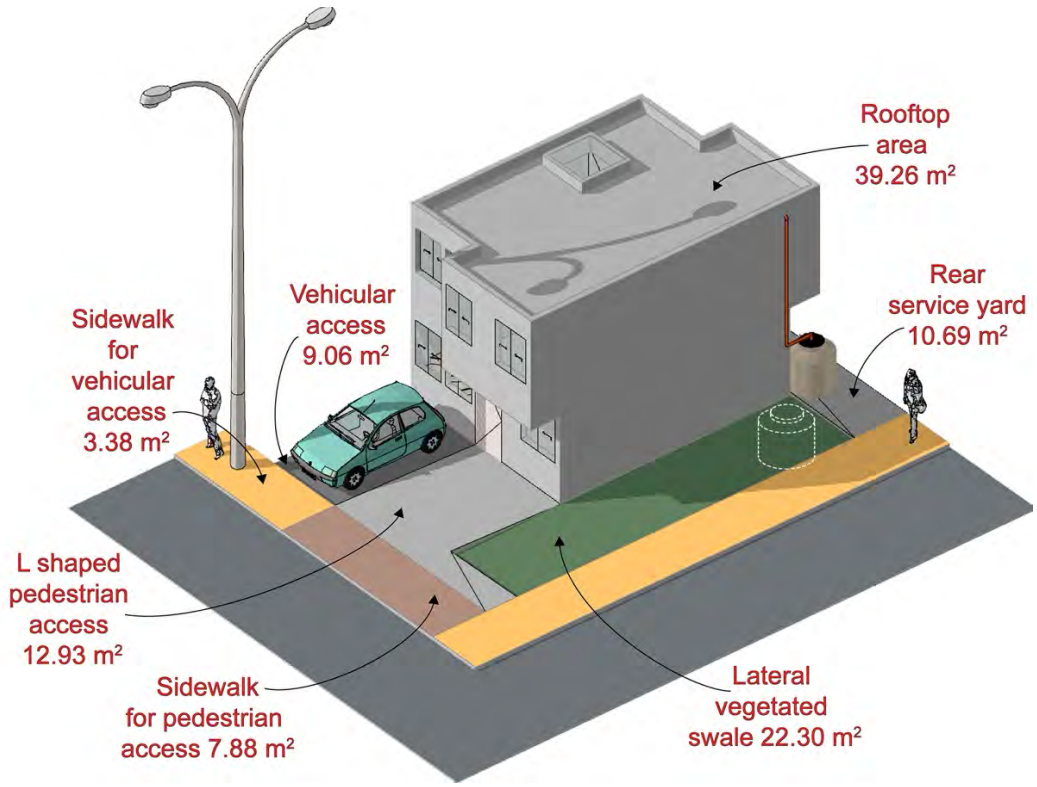

Figure 6. Spatial distribution of impervious surfaces and elements of the BGI prototype in the model house

Water balance of surface runoff collection and treatment

Figure 7 shows a conceptual diagram of runoff water flow through the BGI system for a precipitation event with intensity I (in m/h), accounting for losses due to retention and infiltration at each stage. The water balance is modeled

for three functional units: impermeable sidewalk, permeable pavement, and bioretention cell, before reaching the final storage tank (represented by dotted lines in Figure 7). Unlike traditional systems that favor infiltration into the subsoil, this design aims to maximize water recovery; therefore, both the pavement and the cell are proposed to be waterproofed with a geomembrane. This allows the collected water to be directed entirely to the storage tank, without losses due to deep infiltration. The balance is detailed step by step below.

During rainfall, precipitation first hits the impermeable surface of the sidewalk. This element generates a surface runoff volume of 0.355 m³ per hour, identified as *E*. Of that volume, a small fraction (0.035 m³/h), called *Vret*, is considered lost as it remains retained on the surface. The rest, equivalent to 0.319 m³/h, runs off to the next component of the system: the permeable pavement. This surface runoff flow received from the sidewalk is designated as *Q1*. Simultaneously, the permeable pavement also receives rainwater that falls directly on its surface. This additional volume is estimated at 0.188 m³/h and is identified as *Q2*. Thus, the total volume entering the pavement is the sum of *Q1* and *Q2*, totaling 0.507 m³/h. Within the permeable pavement component, part of the volume infiltrated into the system ($Vinf_1$) and another part advanced through the first porous layer of the pavement without completely infiltrating (V_1 = 0.068 m³/h). Both flows were directed by slope towards the bioretention cell, due to a geomembrane that prevents infiltration into the subsoil.

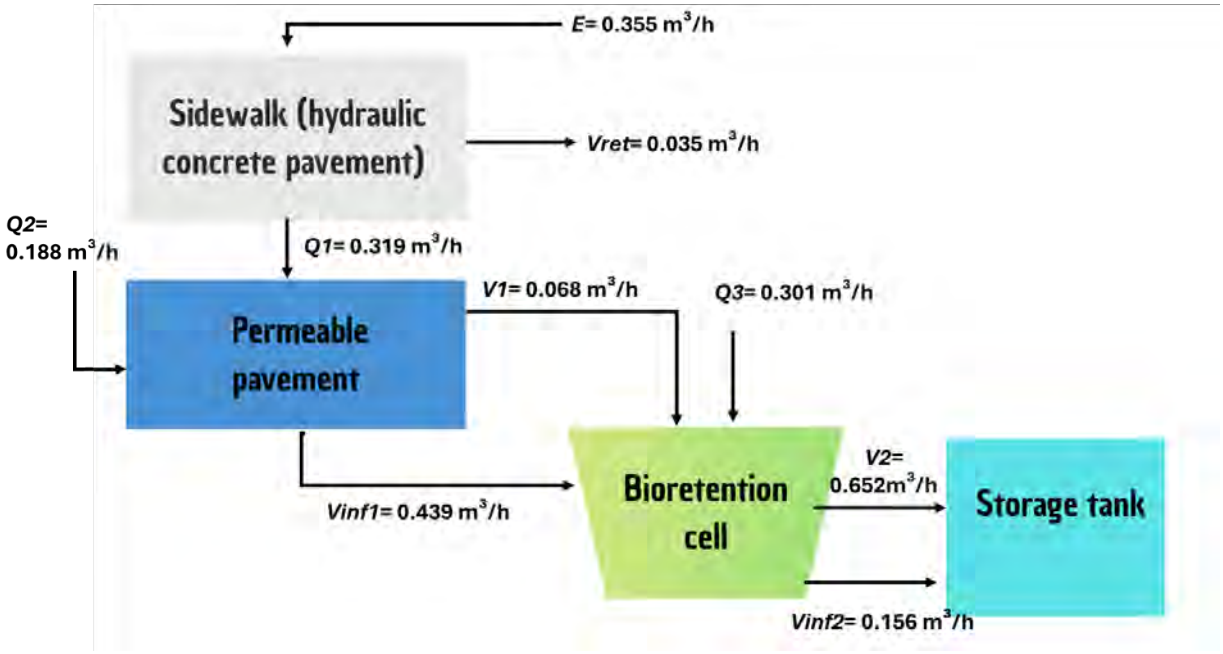

Figure 7. Water balance of the proposed BGI system for the model house

In addition to the flow coming from the pavement, the bioretention cell also captures rainwater that falls directly on its exposed surface. This additional flow, identified as *Q3*, has been estimated at 0.301 m³/h. Thus, the total flow entering the bioretention cell amounts to 0.808 m³/h. Inside the cell, part of the water infiltrates through the deeper layers ($Vinf_2$), while the rest passes through the upper layers and is directed to the storage tank (V_2). In this way, the system uses both the runoff volume and the infiltrated volume to convey water to the storage tank. It is important to note that, possible losses from evaporation from the permeable pavement or evapotranspiration in the bioretention cell have not been considered at this stage, so it is assumed that the entire volume is used for treatment and reuse.

To estimate the flow rates and infiltration volumes, a runoff coefficient of 0.3 was used for the permeable pavement and the bioretention cell, based on the ranges reported by Fletcher *et al.* (2015) for urban drainage systems with green infrastructure. In the specific case of the bioretention cell, an adjusted infiltration coefficient was also applied, obtained by multiplying a vegetation correction factor of 0.7 and a water-substrate contact time of 1 h, in accordance with the methodology proposed by Kasprzyk *et al.* (2022). Finally, a hydraulic conductivity (*K*) of 0.01 m/h for the filter medium was considered, a typical value for soil mixtures with recycled aggregate and vetiver-type vegetation.

Conclusions

This decentralized system proposal, explicitly designed for arid and semi-arid areas, proved to be conceptually feasible by integrating two complementary strategies for rainwater harvesting: direct rooftop collection and surface runoff treatment using blue and green infrastructure. Through simplified water balance calculations, it was estimated that the volumes collected and infiltrated could partially cover domestic non-potable water demand requirements, representing a significant contribution in environments with high water vulnerability. The use of water-saving devices was decisive in reducing per capita consumption and, consequently, improving the relationship between supply and demand. It was assumed that the water collected from the rooftops may meet drinking water quality standards, although further treatment and validation are required. At the same time, the treatment of surface runoff through permeable pavement and bioretention cell seeks to expand its use for non-potable purposes. This differentiation allows prioritizing the potability of the resource collected from roofs and reserving the treated runoff water for other domestic activities, such as irrigation, cleaning, or toilet flushing.

Overall, the results confirm the technical feasibility of a stormwater harvesting, treatment, and storage system at the household level, adaptable to urban contexts with both water and space constraints. This approach represents an effective strategy for moving toward more resilient, decentralized, and environmentally integrated water management.

Acknowledgments and Funding: Dina Margarita Olmedo-Martínez is grateful for the scholarship awarded by the Secretaría de Ciencia, Humanidades, Tecnología e Innovación (SECIHTI, Mexico) to pursue her doctoral studies.

Author contributions: D.M.O.-M.: Conceptualization, Methodology, Investigation, Data curation, Writing – review & editing; C.A.B.-A.: Conceptualization, Investigation, Data curation, Visualization, Writing – review & editing; L.L.-M.: Conceptualization, Investigation, Data curation, Supervision, Writing – review & editing; O.S.A.-R.: Conceptualization, Supervision, Writing – review & editing; M.A.Z.-E.: Conceptualization, Supervision, Writing – review & editing; C.C.-O.: Conceptualization, Supervision, Writing – review & editing; G.A.V.-R.: Conceptualization, Methodology, Supervision, Investigation, Writing – review & editing.

References

Aguirre-Álvarez, E., Lizárraga-Mendiola, L., Coronel-Olivares, C., Tavizón-Pozos, J. A., & Vázquez-Rodríguez, G. A. (2024). Performance of construction and demolition waste coupled with selected vascular plants to treat gray water in nature-based solutions. *Waste and Biomass Valorization, 15*, 5463–5473. https://doi.org/10.1007/s12649-024-02510-7

Anaya-Garduño, M. (2011). *Captación del agua de lluvia: solución caída del cielo*. Biblioteca Básica de Agricultura.

Anderson, A. R., Hunt, W. F., & Smolek, A. P. (2013). Water quality and hydrologic performance of a permeable pavement-modular bioretention treatment train and a stormwater filter box in Fayetteville, North Carolina. *World Environmental and Water Resources Congress 2013: Showcasing the Future*, 3042–3049. https://doi.org/10.1061/9780784412947.296

Beemkumar, N., & Mathews, J. A. (2015). Energy and water consumption analysis of washing process in a fully automatic washing machine. *International Journal of Applied Engineering Research, 10*(11), 10341–10344.

Bigurra-Alzati, C. A., Ortiz-Gómez, R., Vázquez-Rodríguez, G. A., López-León, L. D., & Lizárraga-Mendiola, L. (2021). Water conservation and green infrastructure adaptations to reduce water scarcity for residential areas with semi-arid climate: Mineral de la Reforma, Mexico. *Water, 13*(1), 45. https://doi.org/10.3390/w13010045

Brown, R. A., Skaggs, R. W., Hunt, W. F., & Bean, Z. E. (2012). Hydrologic performance of a permeable pavement–bioretention system in North Carolina, USA. *Water Science and Technology, 66*(7), 1475–1485. https://doi.org/10.2166/wst.2012.341

Carril-Ferreira, J., Costa dos Santos, D., & Campos, L. C. (2024). Blue-green infrastructure in view of integrated urban water management: A novel assessment of an effectiveness index. *Water Research, 257*, 121658. https://doi.org/10.1016/j.watres.2024.121658

Crouch, M. L., Jacobs, H. E., & Speight, V. L. (2021). Defining domestic water consumption based on personal water use activities. *Journal of Water Supply: Research and Technology – AQUA, 70*(7), 1002–1011. https://doi.org/10.2166/aqua.2021.056

Devkota, J., Schlachter, H. E., & Apul, D. S. (2015). Life cycle-based evaluation of harvested rainwater use in toilets and for irrigation. *Journal of Cleaner Production, 95*, 311–321. https://doi.org/10.1016/j.jclepro.2015.01.134

Dobroski, K. (2016). *Exploring feasible domestic water conservation practices*. Washington College. https://doi.org/10.13140/RG.2.1.3666.8404

Fletcher, T. D., Shuster, W., Hunt, W. F., Ashley, R., Butler, D., Arthur, S., & Viklander, M. (2015). SUDS, LID, BMPs, WSUD and more – the evolution and application of terminology surrounding urban drainage. *Urban Water Journal, 12*(7), 525–542. https://doi.org/10.1080/1573062X.2014.916314

Gregory, A. J. (2021). Green stormwater infrastructure for the town of Maynard, MA. *Sustainability Science Working Papers* (No. 1). University of Massachusetts Amherst.

Ismail, A., Shalaby, A.-F., & Khedr, A. (2024). Residential water consumption patterns: a theoretical review. *Environmental Research, Engineering and Management, 80*(3), 251–267. https://doi.org/10.5755/j01.erem.80.3.3687

Kasprzyk, M., Szpakowski, W., Poznańska, E., Boogaard, F. C., Bobkowska, K., & Gajewska, M. (2022). Technical solutions and benefits of introducing rain gardens – Gdańsk case study. *Science of the Total Environment, 835*, 155487. https://doi.org/10.1016/j.scitotenv.2022.155487

Kenway, S. J., Scheidegger, R., & Bader, H.-P. (2019). Dynamic simulation of showers to understand water-related energy in households. *Energy and Buildings, 192*, 45–62. https://doi.org/10.1016/j.enbuild.2019.03.008

Kordana, S., Styś, D., & Dziopak, J. (2014). Rationalization of water and energy consumption in shower systems of single-family dwelling houses. *Journal of Cleaner Production, 82*, 58–69. https://doi.org/10.1016/j.jclepro.2014.06.078

Liu, W., Feng, Q., Chen, W., & Ravinesh, C. (2020). Stormwater runoff and pollution retention performances of permeable pavements and the effects of structural factors. *Environmental Science and Pollution Research, 27*, 30831–30843. https://doi.org/10.1007/s11356-020-09220-2

Lizárraga-Mendiola, L., Vázquez-Rodríguez, G., Blanco-Piñón, A., Rangel-Martínez, Y., & González-Sandoval, M. (2015). Estimating the rainwater potential per household in an urban area: case study in Central Mexico. *Water, 7*(9), 4622–4637. https://doi.org/10.3390/w7094622

Lluch-Cota, S. E., Velázquez-Zapata, J. A., & Nieto-Delgado, C. (2022). Agricultura, agua y cambio climático en zonas áridas de México. *Recursos Naturales y Sociedad, 8*(2), 35–47. https://doi.org/10.18846/renaysoc.2022.08.08.02.0004

Makki, A. A., Stewart, R. A., Panuwatwanich, K., & Beal, C. (2013). Revealing the determinants of shower water end use consumption: enabling better targeted urban water conservation strategies. *Journal of Cleaner Production, 60*, 129–146. https://doi.org/10.1016/j.jclepro.2011.08.007

Otsuka, M., Kouno, S., & Sugimoto, R. (2013). An experimental study on the water-saving effect of water-saving single-lever kitchen faucets. *Journal of Environmental Engineering (Transactions of AIJ), 78*(692), 757–763. https://doi.org/10.3130/aije.78.757

Pakula, C., & Stamminger, R. (2009). Electricity and water consumption for laundry washing by washing machine worldwide. *Energy Efficiency, 3*(4), 365–382. https://doi.org/10.1007/s12053-009-9072-8

Pavlou, P. V., Filippou, S., Solonos, S., Vrachimis, S. G., Malialis, K., Eliades, D. G., Theocarides, T., & Polycarpou, M. M. (2024). Monitoring domestic water consumption: a comparative study of model-based and data-driven end-use classification methods. *Journal of Hydroinformatics, 26*(4), 709–726. https://doi.org/10.2166/hydro.2024.120

Ramírez-Escobar, C. A., & Buriticá-Arboleda, C. I. (2021). Prototipo de cosecha inteligente de agua lluvia para mejorar la eficiencia energética residencial en Bogotá. *Tecnura, 25*(69), 171–195. https://doi.org/10.14483/22487638.17975

Rosas-Flores, J. A., & Morillón-Gálvez, D. (2010). What goes up: recent trends in Mexican residential energy use. *Energy, 35*(6), 2596–2602. https://doi.org/10.1016/j.energy.2010.01.015

Sadr, S. M. K., Memon, F. A., Jain, A., Gulati, S., Duncan, A. P., Hussein, W., Savić, D. A., & Butler, D. (2016). An analysis of domestic water consumption in Jaipur, India. *British Journal of Environment & Climate Change, 6*(2), 97–115. https://doi.org/10.9734/BJECC/2016/23727

Shan, Y., Yang, L., Perren, K., & Zhang, Y. (2015). Household water consumption: insight from a survey in Greece and Poland. *Procedia Engineering, 119*, 1409–1418. https://doi.org/10.1016/j.proeng.2015.08.1001

Tirpak, R. A., Winston, R. J., Simpson, I. M., Dorsey, J. D., Grimm, A. G., Pieschek, R. L., Petrovskis, E. A., & Carpenter, D. D. (2021). Hydrologic impacts of retrofitted low impact development in a commercial parking lot. *Journal of Hydrology, 592*, 125773. https://doi.org/10.1016/j.jhydrol.2020.125773

Vázquez-Rodríguez, G. A., Zúñiga-Estrada, M. A., & Ortiz-Hernández, J. E. (2024). Blue and green infrastructure: history and experiences in Mexico and the arid and semi-arid global south. In *Sustainable spaces in arid and semiarid zones of Mexico* (pp. 69–89). Springer International Publishing.

Wilkes, C. R., Mason, A. D., & Hern, S. C. (2005). Probability distributions for showering and bathing water-use behavior for various US subpopulations. *Risk Analysis, 25*(2), 317–337. https://doi.org/10.1111/j.1539-6924.2005.00592.x

Willis, R. M., Stewart, R. A., Panuwatwanich, K., Jones, S., & Kyriakides, A. (2010). Alarming visual display monitors affecting shower end use water and energy conservation in Australian residential households. *Resources, Conservation & Recycling, 54*(12), 1117–1127. https://doi.org/10.1016/j.resconrec.2010.03.004

Zúñiga-Estrada, M. A., Lizárraga-Mendiola, L., Ramírez-Cardona, M., & Vázquez-Rodríguez, G. A. (2024). Biomineralization of urban runoff pollutants in bioretention cells adapted to hot semi-arid climates. *Earth Systems and Environment, 8*, 1699–1711. https://doi.org/10.1007/s41748-024-00487-w

An Integrated Modeling Approach for Biogas Production from Anaerobic Co-Digestion of Cattle Manure and Tomato Waste

Guillermo Benítez Olivares [1,*], Alejandro Torres Aldaco [1], Raúl Lugo Leyte [1], Helen Denise Lugo Méndez [2], Vianka Celina Hernández-Fydrych [3]

[1] Departamento de Ingeniería de Procesos e Hidráulica, Universidad Autónoma Metropolitana-Iztapalapa, Av. Ferrocarril San Rafael Atlixco No. 186, Colonia Leyes de Reforma 1ª Sección, 09310, Alcaldía Iztapalapa, Ciudad de México, México.
[2] Departamento de Procesos y Tecnología, Universidad Autónoma Metropolitana-Cuajimalpa, Av. Vasco de Quiroga No. 4871, Colonia Santa Fe Cuajimalpa, 05348, Cuajimalpa, Ciudad de México, México.
[3] Departamento de Ciencias Básicas, Universidad Autónoma Metropolitana-Azcapotzalco, Av. San Pablo Xalpa 180, San Martin Xochinahuac, Alcaldía Azcapotzalco, 02128, Ciudad de México, México
* Corresponding author: gbenitez@izt.uam.mx; Tel.: (5558044600#1239)

Received: February 11, 2026 Accepted: May 2, 2026 Published: May 28, 2026
DOI: https://doi.org/10.56845/rebs.v8i2.685

Abstract: This study develops and validates a multi-scale modeling framework to estimate biogas production from the anaerobic co-digestion (AcoD) of cattle manure and tomato crop waste (*Solanum lycopersicum L.*), an abundant and underutilized agricultural residue in Mexico. The modeling approach integrates three complementary mathematical models (Volume Averaging, Laplace Domain, and Modified Gompertz equation) which were fitted to experimental data previously reported in the literature. These data were obtained from batch bioreactors experiments conducted under different operational conditions (20% and 50% substrate on a dry basis, and pH 6.8 and 7.5). The models exhibited a strong fit (R^2: 0.84 – 0.97; RMSE = 0.10 – 1.10), supporting their suitability for describing both kinetic and transport phenomena. The Volume Averaging method enabled the estimation of transport parameters, including diffusion coefficients on the order of 1.6×10−6 m²/d, along with key reaction parameters. The Laplace Domain approach facilitated the dynamic characterization of the system through transfer functions, while the Modified Gompertz equation accurately captured biogas production kinetics. The results indicate that operating at 50% substrate concentration with pH control reduced the characteristic production time to approximately 30 days, which is less than half the time required for the 20% substrate condition (60-66 days) and achieved methane contents of up to 41%, approaching the established threshold for biogas as biofuel (45%), with V50a showing the highest methane fraction. The estimated kinetic and transport coefficients suggest a clear metabolic adaptation of the microbial consortia under optimal conditions. Overall, this integrated framework demonstrated its potential for the design and scale-up of AcoD systems, providing a link between physicochemical fundamentals and practical application in agricultural regions with high organic waste generation.

Keywords: biogas modeling, agricultural waste valorization, anaerobic co-digestion, tomato waste, sustainable energy

Nomenclature

Symbol	Description	Units
Latin Symbols		
A_ζ	Stimulus amplitude	d
c_A	Concentration of species A in the bioreactor volume	mol/m³
$\langle c_A \rangle$	Average concentration of species A	mol/m³
$\mathcal{D}_A$	Effective diffusion coefficient of gaseous species A	m²/d
d_R	Reactor diameter	m
k_p	Concentration divided by the characteristic time	mol/(m³·d)
L_R	Reactor length	m
R^2	Coefficient of determination	–
$RMSE$	Root Mean Square Error	L
s	Frequency domain variable (Laplace)	d⁻¹
t	Time	d
V_R	Reactor volume	m³
Greek Symbols		
α_A	Reactor properties divided by the volume fraction $(\alpha_A = L_R \mathcal{D}_A (\varepsilon V_R)^{-1})$	d⁻¹
ε	Volume fraction occupied in the bioreactor	–
κ_{eff}	Effective Michaelis-Menten saturation constant	mol/m³
λ_ψ	Lag phase in the Gompertz equation	d
μ_{eff}	Maximum effective reaction rate	mol/(m³·d)
μ_{A}	Reaction rate divided by the volume fraction $(\mu_{\text{A}} = \mu_{\text{eff}} \varepsilon^{-1})$	mol/(m³·d)
$\mu_{\text{max},\psi}$	Maximum specific production rate of biogas or methane	L/(gVS·d)
ψ_0	Specific maximum production potential	L/(gVS·d)
τ_p	Characteristic time of the process	d

Symbol	Description
Subscripts	
A	Species (Biogas or Methane)
eff	Effective
max	Maximum
R	Reactor
$V20, V50$	20% or 50% dry basis
a, b	pH conditions (a: 6.8, b: 7.5)
Acronym	**Description**
Abbreviations	
AD	Anaerobic Digestion
AcoD	Anaerobic Co-Digestion
BMP	Biochemical Methane Potential
COD	Chemical Oxygen Demand
TS	Total Solids
VS	Volatile Solids
VFA	Volatile Fatty Acids

Introduction

The global search for sustainable energy sources has positioned biogas as a key renewable fuel, particularly in agricultural regions where organic waste is abundant (Alghoul *et al*., 2019; Kumar and Samadder, 2020). In Mexico, approximately 13% of the workforce is dedicated to agriculture, generating significant amounts of organic residues that are generally disposed of without treatment (Mendivil-Garcia *et al*., 2020). This situation represents both an environmental challenge and an energy opportunity, especially considering that about one-third of the world's food production is wasted annually (Kumar and Samadder, 2020).

Anaerobic Digestion (AD) has become a promising technology for converting organic waste into biogas while contributing to the reduction of greenhouse gas emissions (Alburquerque *et al*., 2012; Kumar and Samadder, 2020; Elagroudy *et al*., 2020). The economic and energy interest in biogas lies in its methane fraction (CH_4), which constitutes between 50% and 70% of its composition and defines its calorific value. Therefore, the carbon-to-methane conversion efficiency is a critical parameter for the sustainability and profitability of the process (Börjesson and Mattiasson, 2008; Chaemchuen *et al*., 2016). In this context, the anaerobic co-digestion (AcoD) of animal manure with agricultural residues has been shown to improve both methane production and system stability, thanks to synergistic interactions between substrates (Esposito *et al*., 2012; Castro-Rivera *et al*., 2020). Among potential substrates, tomato crop waste (*Solanum lycopersicum L.*) is particularly attractive due to its high organic content and seasonal availability in farming areas (Castro-Rivera *et al*., 2020). In Mexico, where tomato production generates approximately 1.8 million tons of waste annually (SIAP, 2023), the energy valorization of these by-products represents a strategic opportunity to contribute to national energy transition goals (SENER, 2020). However, full-scale implementation requires modeling tools that capture both kinetic and transport phenomena.

Mathematical modeling plays an essential role in understanding, optimizing, and scaling up AD processes (Hatata *et al*., 2021; Benítez-Olivares *et al*., 2016). Although various approaches exist, from complex kinetic models (Esposito *et al*., 2012; Hernández-Fydrych *et al*., 2021) to empirical formulations like the Gompertz equation (Zwietering *et al*., 1990), a gap persists in developing integrated frameworks that link fundamental transport phenomena with practical production kinetics. Most previous studies have focused on individual approximations; for example, Ravina *et al*. (2019) developed MATLAB software for biogas quantification; Nock *et al*. (2014) used mass transfer models to optimize biogas quality; and Hernández-Fydrych *et al*. (2019) applied kinetic models to slaughterhouse wastewater treatment.

The methodological novelty of this work lies in the synergistic integration of three complementary modeling perspectives: volume averaging to capture fundamental micro-scale transport phenomena, analysis in the Laplace domain to characterize the system's temporal dynamics, and the modified Gompertz equation to describe practical production kinetics. While previous studies have applied these methods in isolation (Ravina *et al*., 2019; Nock *et al*., 2014; Hernández-Fydrych *et al*., 2019), their combination into a unified framework overcomes the limitations of each individual approach, particularly for AcoD systems where synergistic substrate interactions introduce complex non-linearities (Esposito *et al*., 2012). This multi-scale approach provides not only kinetic parameters but also fundamental transport coefficients critical for bioreactor scale-up, an aspect often underestimated in the literature (Whitaker, 1999; Benítez-Olivares *et al*., 2016).

The main objectives of this work are:

1. To develop and validate an integrated multi-scale modeling framework that combines Volume Averaging, Laplace Domain, and Modified Gompertz approaches for biogas production from the AcoD of cattle manure and tomato crop waste.
2. To determine effective transport coefficients (diffusion coefficients $\mathcal{D}_A$, reaction rates μ_{eff}, and saturation constants κ_{eff}) under different operational conditions and establish their relationship with system performance.
3. To validate a multi-scale model for estimating biogas from AcoD of agricultural residues in developing regions.

Materials and Methods

Experimental System Description

This study is based on experimental data previously published by Castro-Rivera *et al*. (2020), obtained from a laboratory-scale system for biogas production through AcoD of cattle manure and tomato agricultural waste (*Solanum lycopersicum L.*). These data were used exclusively for analysis and mathematical modeling purposes, without conducting new experimental tests. In the original study (Castro-Rivera *et al*., 2020), experiments were conducted in 3 L plastic digesters with a working volume of 2.4 L and a 10% total solids concentration on a dry basis. The characterization of substrates (cattle manure and tomato peel) and effluents included determinations of chemical composition, pH, chemical oxygen demand (COD), total solids (TS), volatile solids (VS), substrate-to-inoculum ratio, alkalinity, and digestion time. A complete description of the experimental conditions is detailed in the original source (Castro-Rivera *et al*., 2020).

Briefly, in the reference work, each biodigester had a gas outlet and a liquid outlet for sampling. Before hermetic sealing, a nitrogen purge was performed for five minutes to remove dissolved oxygen and ensure anaerobic conditions. The digesters were maintained for 75 days at 30°C. Weekly, the biogas volume was measured according to the procedure described in Castro-Rivera *et al*. (2020), and its composition (CH_4 and CO_2) was determined by gas chromatography. The experimental design was completely randomized, with a factorial arrangement (2×2) and three replicates per treatment. The evaluated factors were the mixture of manure with tomato peel in proportions of 20/80% and 50/50% respectively, and the initial pH (6.8 and 7.5). For the purposes of the present modeling work, the corresponding data were grouped into four case studies:

- **V20a**: 20% dry basis, pH = 6.8
- **V20b**: 20% dry basis, adjusted pH = 7.5
- **V50a**: 50% dry basis, pH = 6.8
- **V50b**: 50% dry basis, adjusted pH = 7.5

From these data, three complementary mathematical models were implemented and evaluated to represent and analyze the behavior of biogas production and its methane fraction. The models considered were the Volume Averaging model, the Laplace Domain model, and the Modified Gompertz equation. Figure 1 illustrates the multi-scale modeling strategy implemented, integrating different levels of process description.

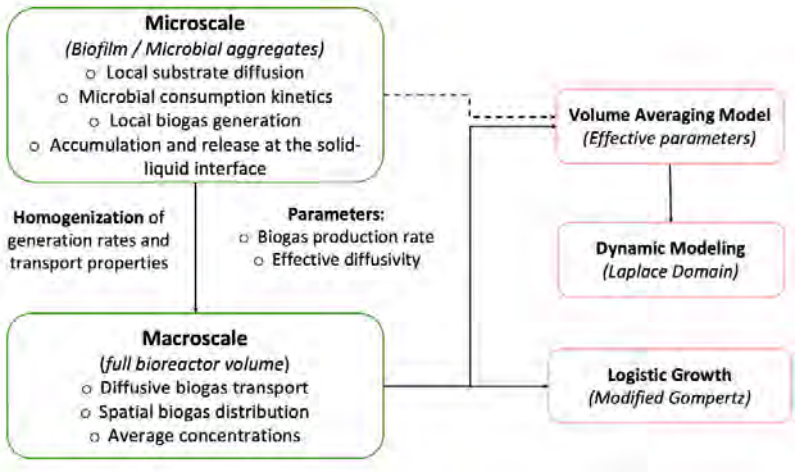

Figure 1. Schematic of the multi-scale modeling strategy implemented in this work

Mathematical Models

To adequately represent the formation and transport of biogas within the bioreactor, a multi-scale modeling strategy was developed that integrates local reaction and diffusion phenomena with the global system dynamics. The approach

is based on a conceptual separation between a micro-scale, where biochemical and transport processes occur within biofilms and microbial aggregates, and a macro-scale, which describes the behavior of biogas in the total reactor volume.

At the micro-scale, the species of interest is the local concentration of biogas generated from microbial reactions. This stage explicitly considers the phenomena of substrate diffusion towards microbial structures, biochemical consumption via microbial kinetics, and localized biogas production. Additionally, the accumulation and release of gas at the solid-liquid interface is incorporated, allowing the capture of the intrinsic spatial heterogeneity of reactive microenvironments (Picioreanu *et al*., 1998).

The local biogas production rates and transport parameters obtained undergo a homogenization process, through which they are transformed into effective properties representative of the active reactor volume. These variables include the effective volumetric biogas generation rate, effective diffusivity, and other coefficients associated with gas transport and release.

At the macro-scale, these homogenized properties are incorporated into a model that describes the reactor dynamics and biogas transport at a global level. This model considers the effects of mixing, fluid circulation, bubble formation, as well as the diffusive transport of gas throughout the bioreactor volume. In this way, it is possible to predict the spatial distribution of biogas, its concentration gradients, and its accumulation or release during operation (Bird, Stewart, & Lightfoot, 2002; Velázquez-Martí *et al*., 2018).

Finally, a sequential coupling is established between both scales, where parameters estimated from the micro-scale (Volume Averaging model) serve as inputs for the macro-scale Laplace domain model. This ensures consistency between the fundamental transport phenomena and the global system dynamics.

Volume Averaging Model

The first model is based on the Volume Averaging method (Whitaker, 1999), which allows deriving transport equations at the bioreactor scale from the equations governing transport at the micro-scale. This approach considers three scale levels (Figure 2): the micro-scale ($r_{\beta\sigma}$), where microbial interactions occur; the intermediate region ($r_{\kappa\gamma}$); and the bioreactor scale.

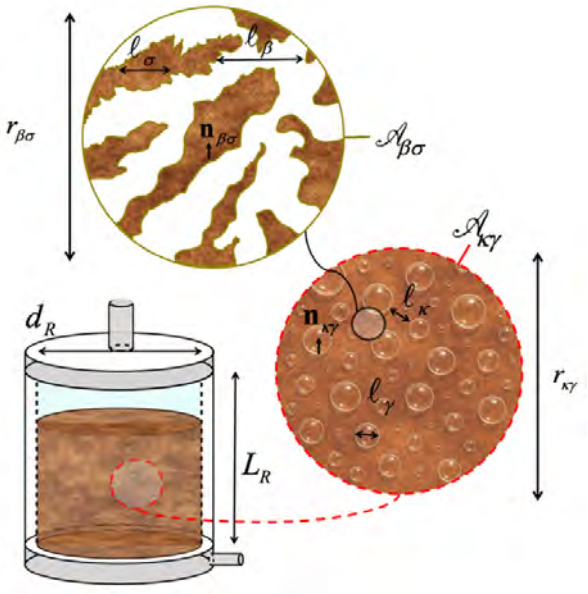

Figure 2. Diagram of the biodigester and the scaling used for the digestion of cattle manure and tomato crop waste. Where $r_{\beta\sigma}$ schematizes microbial interactions; $r_{\kappa\gamma}$ schematizes mass transport; d_R and L_R are the diameter and length of the reactor, respectively. Adapted from Castro-Rivera *et al*., 2020

Following the methodology established by Ochoa *et al*. (1986) and Benítez-Olivares *et al*. (2016), the volume averaging operator was applied to obtain a macroscopic mass transfer equation describing the accumulation of biogas in the bioreactor:

$$\varepsilon \frac{\partial \langle c_A \rangle}{\partial t} = \mathcal{D}_A \frac{\partial^2 \langle c_A \rangle}{\partial z^2} + \frac{\mu_{\text{eff}} \langle c_A \rangle}{\kappa_{\text{eff}} + \langle c_A \rangle} \quad \textbf{(1)}$$

where $\langle c_A \rangle$ is the average concentration of species *A* (biogas or methane) in [mol/m³], ε is the volume fraction occupied in the reactor, $\mathcal{D}_A$ is the effective diffusion coefficient in [m²/d], μ_{eff} is the maximum effective reaction rate in [mol/(m³·d)], and κ_{eff} is the Michaelis-Menten saturation constant in [mol/m³]. To consider the process throughout the reactor volume, the averaging operator is applied:

$$c_A = \frac{1}{V_R} \int_{V(t)} \langle c_A \rangle dV \quad \textbf{(2)}$$

obtaining the ordinary differential equation:

$$\varepsilon \frac{\partial c_A}{\partial t} = \frac{L_R}{V_R} \mathcal{D}_A c_A + \frac{\mu_{\text{eff}} c_A}{\kappa_{\text{eff}} + c_A} \quad \textbf{(3)}$$

The numerical solution of Equation 3 was implemented in MATLAB using both the Runge-Kutta method and the finite difference method, allowing the determination of the transport coefficients $\mathcal{D}_A$, μ_{eff}, and κ_{eff}.

Model in the Laplace Domain

The second model is developed in the Laplace domain, providing an alternative approach to characterize system dynamics through transfer functions. Starting from Equation 3 and defining where $\alpha_A = L_R \mathcal{D}_A (\varepsilon V_R)^{-1}$ and $\mu_{\text{A}} = \mu_{\text{eff}} \varepsilon^{-1}$, we obtain:

$$\frac{dc_A}{dt} = \alpha_A c_A \frac{\mu_{\text{A}} c_A}{\kappa_{\text{eff}} + c_A} \quad \textbf{(4)}$$

The nonlinearity in the reaction term is linearized using a first-order Taylor expansion around an operating point $\bar{c}_A$:

$$f[c_A(t)] \approx f(\bar{c}_A) + \frac{df}{dc_A}[c_A(t) - \bar{c}_A] \quad \textbf{(5)}$$

Applying the Laplace transform (Widder, 2015),

$$k_p X(t) = \frac{\bar{c}_A}{\tau_p} \left[\frac{\mu_{\text{A}} \kappa_{\text{eff}}}{(\kappa_{\text{eff}} + \bar{c}_A)^2} - \frac{\mu_{\text{A}}}{\kappa_{\text{eff}} + \bar{c}_A} \right] \quad \textbf{(6)}$$

we obtain the standard form in the Laplace domain:

$$\tau_p \frac{dc_A}{dt} + c_A = k_p X(t) \quad \textbf{(7)}$$

whose Laplace transform results in:

$$\tilde{\zeta}_A = \frac{k_p}{\tau_p \left(s + \frac{1}{\tau_p} \right)} \tilde{\xi} \quad \textbf{(8)}$$

Where $\tilde{\zeta}_A = \mathcal{L}(\tilde{c}_A)$ and $\tilde{\xi} = \mathcal{L}(\tilde{X})$ are the variables in the Laplace domain, s [d^{-1}] is the frequency variable, τ_p [d] is the characteristic time of the process, and k_p [mol/(m^3·d)] condenses the concentration and reaction terms. Applying the inverse transform with $\tilde{\xi} = \frac{A_\zeta}{s}$, where A_ζ [d] is the stimulus amplitude, the temporal solution is obtained:

$$\tilde{\zeta}_A = A_\zeta k_p \left(1 - \exp^{-t/\tau_p}\right) \quad \textbf{(9)}$$

This equation provides an explicit relationship for cumulative biogas production as a function of time.

Modified Gompertz Equation

The third model employs the modified Gompertz equation (Zwietering *et al*., 1990), widely used to describe methane production kinetics in Biochemical Methane Potential (BMP) assays:

$$\psi(t) = \psi_0 \exp\left\{-\exp\left[\frac{\mu_{\max,\psi} \cdot e(1)}{\psi_0}(\lambda_\psi - t) + 1\right]\right\} \quad \textbf{(10)}$$

where $\psi(t)$ [L/gVS] is the accumulated biogas produced at time t, ψ_0 [L/gVS] is the maximum specific production potential, $\mu_{\max,\psi}$ [L/(gVS·d)] is the maximum specific production rate, and λ_ψ [d] is the lag phase.

While the lag phase was found to be negligible in most of our fitted cases, the Gompertz model was retained for three reasons: (1) it is the standard model in BMP assays, ensuring comparability with literature; (2) the three-parameter form provides slightly better fit during the transition from the initial to the exponential phase compared to two-parameter models like the logistic; and (3) the lag phase parameter, even when near zero, serves as a useful diagnostic indicator of rapid microbial adaptation. Nevertheless, we acknowledge that for systems consistently showing no lag, simpler first-order or logistic models could be equally valid and more parsimonious.

Numerical Implementation Strategy

Numerical implementation was carried out through algorithms developed in MATLAB that integrate the three modeling approaches:

- For the Volume Averaging model (Eq. 3), numerical methods for differential equations (Runge-Kutta and finite differences) were used.
- For the Laplace (Eq. 9) and Gompertz (Eq. 10) models, nonlinear regression was employed to estimate parameters by minimizing the mean square error.
- The coefficients obtained from the Volume Averaging model served as initial values for the Laplace model adjustment, establishing a connection between both approaches.
- The value of the volume fraction was kept constant at ε =0.8 for all cases, corresponding to the ratio between the reactor volume and the added organic matter.

Results and Discussion

This section presents the validation of the three proposed mathematical models against the experimental data of biogas production and its corresponding CH_4 fraction for the four case studies. The analysis focuses on the models' predictive capacity, the estimation of process parameters, and the effect of operational conditions on system performance.

Comparative Performance of the Modeling Approaches

The cumulative production values reported here (e.g., 2.4 L/gVS for V20a biogas) represent the total measured production over 75 days. The Gompertz parameter ψ_0 reported in Tables 1-4 represents the model-fitted asymptotic maximum, which may be slightly higher.

Figures 3 to 6 show the comparison between experimental data and predictions for biogas and methane production for the different case studies. In all scenarios, a qualitative and quantitative agreement between the modeled curves and experimental data is observed.

As observed in Figure 3, experiment V20a (20% substrate, pH 6.8) showed a prolonged period of very slow production, which could be visually interpreted as a latency phase. However, model fitting indicated a negligible statistical lag phase, suggesting this behavior is due to extremely slow kinetic rates rather than a true biological adaptation period. This low generation could be attributed to the microorganisms' adaptation period to the new substrate, which slowed the microbial growth rate, coupled with possible accumulation of volatile fatty acids (VFAs) that would have inhibited metabolic activity (Khadka *et al*., 2022). This behavior coincides with that reported by Esposito *et al*. (2012), who observed that suboptimal substrate concentrations, in combination with acidic pH, significantly reduce the metabolic activity of methanogenic consortia. Under these characteristics, the methane/biogas ratio was approximately 27%, a value below the 45% threshold proposed to consider biogas as a viable biofuel (Dueblein and Steinhauser, 2008), evidencing inefficient substrate conversion.

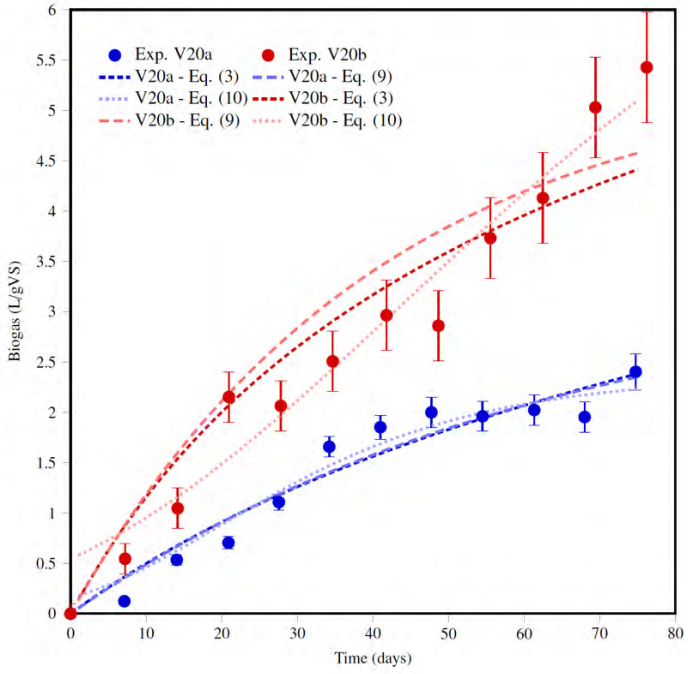

Figure 3. Cumulative biogas production for experiments V20a and V20b (20% manure on dry basis, pH = 6.8 and adjusted pH = 7.5, respectively). Points represent experimental values with error bars indicating observed variability. Lines show the fits of the three mathematical models: Volume Averaging (Eq. 3), Laplace Domain (Eq. 9), and Modified Gompertz (Eq. 10)

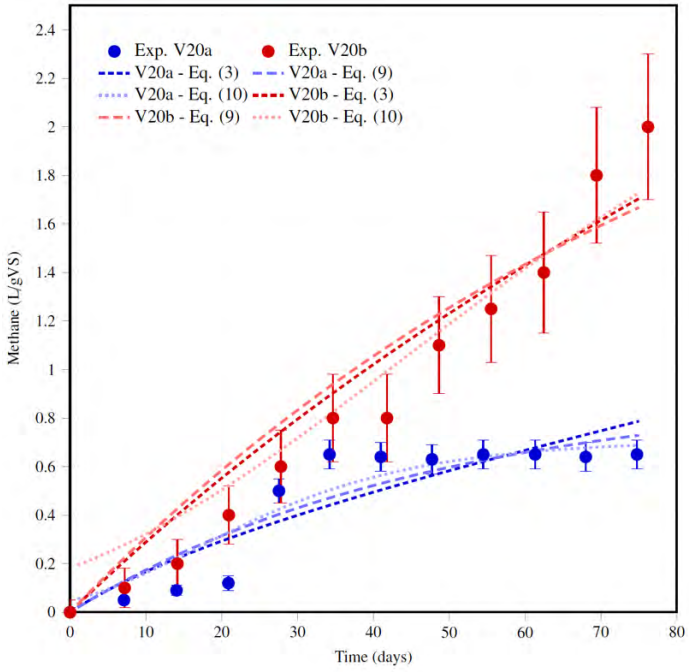

Figure 4. Cumulative methane production for experiments V20a and V20b (20% manure on dry basis, pH = 6.8 and adjusted pH = 7.5, respectively). Points represent experimental values with error bars indicating observed variability. Lines show the fits of the three mathematical models

pH control at 7.5 in experiment V20b (a) resulted in a 125% increase in biogas production compared to V20a. Under these conditions, a yield of 5.4 L/gVS of biogas was obtained, of which 2.0 L/gVS corresponded to CH_4. This increase could be attributed to greater microbial activity, as pH levels close to neutrality favor the balance of microbial consortia (Hernández-Fydrych *et al*. 2019). However, despite the increase in total biogas production, the methane/biogas ratio was only 37%. This value suggests that, although neutral pH increased metabolic activity, the 20% substrate concentration continued to be a limitation for conversion to CH_4, preventing achievement of the minimum percentage required to consider this biogas as a biofuel (González-Herrera *et al*. 2021).

In Figures 5 and 6 (V50a and V50b, respectively), the increase in substrate to 50% with improvements in system performance is observed. In V50a (pH 6.8), biogas production reached 8.1 L/gVS with a methane/biogas ratio of 41%, a value close to the 45% threshold. This behavior agrees with that reported by Castro-Rivera *et al*. (2020), who indicated that elevated substrate concentrations provide the necessary nutrient bioavailability to maintain robust microbial

activity even under suboptimal pH conditions. It is particularly relevant that V50a surpassed V20b in CH_4 conversion efficiency, evidencing that a higher substrate concentration can partially compensate for pH limitations (Li *et al*. 2022).

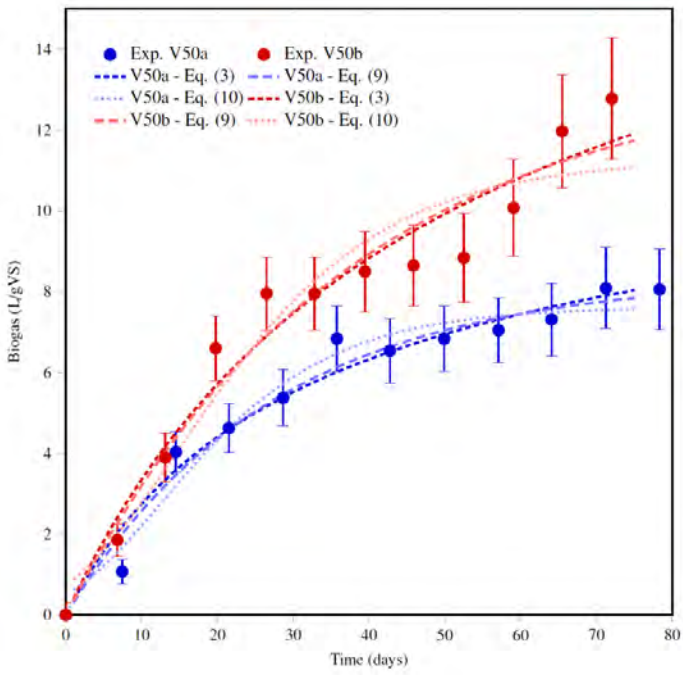

Figure 5. Cumulative biogas production for experiments V50a and V50b (50% manure on dry basis, pH = 6.8 and adjusted pH = 7.5, respectively). Points represent experimental values with error bars indicating observed variability. Lines show the fits of the three mathematical models

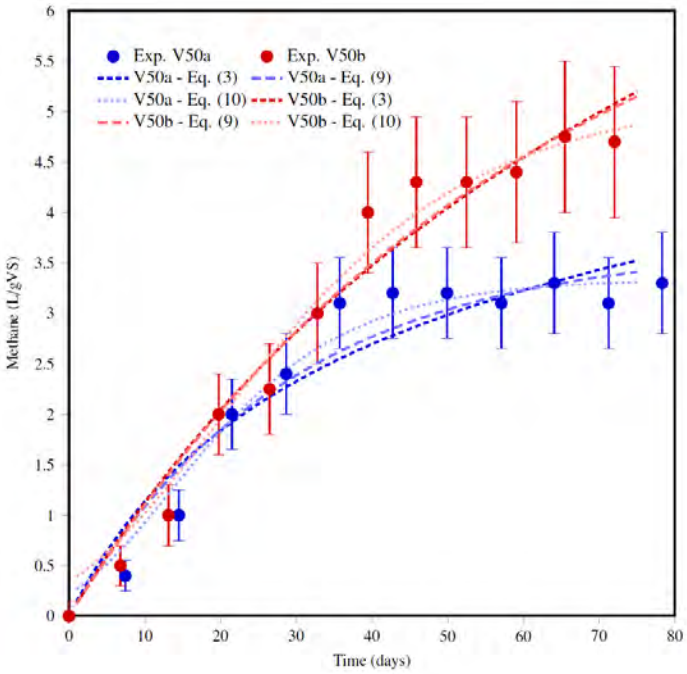

Figure 6. Cumulative methane production for experiments V50a and V50b (50% manure on dry basis, pH = 6.8 and adjusted pH = 7.5, respectively). Points represent experimental values with error bars indicating observed variability. Lines show the fits of the three mathematical models

The combination of high substrate load (50%) with pH control (7.5) in V50b produced the maximum biogas generation of the study: 12.8 L/gVS of biogas and 4.75 L/gVS of methane. However, the methane/biogas ratio decreased to 37% compared to V50a. This apparent discrepancy can be attributed to the accumulation of volatile fatty acids and degradation intermediates, as suggested by Kumar and Samadder (2020) for systems with high organic load, where CO_2 production tends to increase disproportionately. Nevertheless, the absolute methane content in V50b (4.75 L/gVS) significantly exceeded that of V50a (3.3 L/gVS), making V50b the optimal condition when the objective is to maximize total energy production.

In all cases, the coefficients of determination (R^2) ranged from 0.84 to 0.97, while the root mean square errors (RMSE) varied from 0.10 to 1.10 L. The Volume Averaging model systematically obtained the best fits (highest R^2 and lowest RMSE), which could be due to its basis in fundamental physical principles. However, the Laplace and Gompertz models provided useful representations with specific computational advantages.

Determined transport and kinetic parameters

Tables 1 to 4 present the values of transport and kinetic coefficients obtained by fitting the models to the data in Figures 3 to 6, respectively.

The effective diffusion coefficients ($\mathcal{D}_A$) obtained in this work, on the order of 1.6×10^{-6} m²/d (equivalent to ~1.85×10^{-11} m²/s), are of significant interest. These values show a remarkable correspondence with those reported for high-solids anaerobic digestion media. Specifically, our modeled values align closely with those determined experimentally by Gooddy *et al*. (2007) for digestates with total solids (TS) contents above 15%. In that study, effective diffusivity values for iodide in media with 15%, 19%, and 25% TS were in the range of 1.00 to 1.12×10^{-11} m²/s, converging toward a lower limit near 10^{-11} m²/s as solids concentration increased. This similarity, despite

methodological differences (diffusion of an ionic solute vs. modeling of methane and biogas gas transfer), is highly significant. It validates the proposed modeling tools (Volume Averaging and Laplace transform) as robust methods for estimating transport parameters in complex media, as they successfully reproduce the same order of magnitude of diffusivity obtained through direct experimental techniques. Furthermore, it confirms that in co-digestion systems such as the one studied here (cattle-tomato), the effective diffusivity is severely restricted by the tortuosity and microstructure of the porous medium, reaching values comparable to highly restrictive media like sedimentary rocks, rather than typical free aqueous media (~10^{-9} m²/s). This consistency underscores that the main physical limitation for mass transfer in these systems is not the intrinsic molecular diffusion, but the architecture of the digestate medium, dominated by capillary and bound water, as explained by Gooddy *et al*. (2007). The slight difference observed between biogas and methane $\mathcal{D}_A$ values can be attributed to variations in the molecular diffusion coefficients specific to each gaseous species, as documented by Whitaker (1999) for multiphase systems.

Regarding kinetic parameters, the values of μ_{eff} and κ_{eff} show clear differences between experimental conditions. In V20 systems, the elevated values of κ_{eff} (79.63 - 85.42 mol/m³ for biogas) indicate a lower affinity of the microbial consortia for the substrate, implying the need for higher concentrations to reach half of the maximum reaction rate (Khadka *et al*., 2022). This behavior coincides with that reported by Zwietering *et al*. (1990), who associated high saturation constants with limitations in nutrient bioavailability. In contrast, in V50 systems, a notable reduction in κ_{eff} (29.06-32.15 mol/m³) was observed, suggesting greater metabolic adaptation and more efficient substrate utilization, possibly favored by greater availability of co-substrates that stimulate synergies in anaerobic degradation pathways (Li *et al*. 2022).

Table 1. Transport and kinetic parameters for V20 experiments for biogas yield

Parameter	Exp. V20a	Exp. V20b
$\mathcal{D}_A$ (m²/d)	1.62×10⁻⁶	1.65×10⁻⁶
μ_{eff} (mol/m³·d)	4.23	5.67
κ_{eff} (mol/m³)	79.63	85.42
τ_p (d)	60.2	65.7
A_ζ (d)	1.89	2.49
k_p (mol/m³·d)	1.76	2.74
ψ_0 (L/gVS)	0.245	0.312
$\mu_{\max,\,\psi}$ (L/gVS·d)	0.018	0.022

Table 2. Transport and kinetic parameters for V20 experiments for methane yield

Parameter	Exp. V20a	Exp. V20b
$\mathcal{D}_A$ (m²/d)	1.58×10⁻⁶	1.61×10⁻⁶
μ_{eff} (mol/m³·d)	1.45	2.12
κ_{eff} (mol/m³)	27.76	75.34
τ_p (d)	59.8	66.3
A_ζ (d)	1.03	1.52
k_p (mol/m³·d)	1.02	1.53
ψ_0 (L/gVS)	0.082	0.105
$\mu_{\max,\,\psi}$ (L/gVS·d)	0.004	0.011

The analysis of characteristic times (τ_p) reveals a fundamental difference between low and high substrate concentration systems. While V20 experiments recorded τ_p values between 60 and 66 days, V50 systems showed times of 30 to 31 days, representing a 50% reduction in the period required to reach maximum production. This kinetic acceleration can be explained by the substrate limitation theory proposed by Monod (Monod, 1949), according to which higher initial concentrations decrease the time necessary for microbial populations to reach their maximum metabolic activity.

The values of A_ζ and k_p obtained from the Laplace model support these accelerated dynamics, with increases of 89% in A_ζ and 135% in k_p when comparing V20a with V50b.

Likewise, the parameters of the Gompertz equation $(\psi_0;\ \mu_{\max,\,\psi})$ show some improvements under optimal conditions. The maximum specific production potential ψ_0 increased by 113% for biogas and 166% for methane between V20a and V50b, while the maximum specific rate $\mu_{\max,\,\psi}$ increased by 72% and 150%, respectively. These results are consistent with those reported by Esposito *et al*. (2012), who described synergistic effects in AcoD due to the nutritional complementarity between cattle manure and vegetable residues, favoring an optimal nutrient balance for microbial consortia. The ratio $\psi_{\text{biogas}}/\psi_{\text{CH}_4}$ decreases from 2.99 in V20a to 2.40 in V50b, indicating a more efficient conversion of substrate to methane under conditions of higher substrate concentration.

Table 3. Transport and kinetic parameters for V50 experiments for biogas yield

Parameter	Exp. V50a	Exp. V50b
$\mathcal{D}_A$ (m²/d)	1.64×10^{-6}	1.67×10^{-6}
μ_{eff} (mol/m³·d)	6.89	8.45
κ_{eff} (mol/m³)	29.06	32.15
τ_p (d)	30.5	31.2
A_ζ (d)	2.62	3.58
k_p (mol/m³·d)	1.46	3.43
ψ_0 (L/gVS)	0.412	0.523
$\mu_{\max,\,\psi}$ (L/gVS·d)	0.024	0.031

Table 4. Transport and kinetic parameters for V50 experiments for methane yield

Parameter	Exp. V50a	Exp. V50b
$\mathcal{D}_A$ (m²/d)	1.59×10^{-6}	1.63×10^{-6}
μ_{eff} (mol/m³·d)	3.12	4.78
κ_{eff} (mol/m³)	29.63	58.27
τ_p (d)	29.8	30.7
A_ζ (d)	3.19	1.63
k_p (mol/m³·d)	2.73	3.12
ψ_0 (L/gVS)	0.198	0.218
$\mu_{\max,\,\psi}$ (L/gVS·d)	0.010	0.010

Effect of substrate concentration

Substrate concentration proved to be a critical factor in system performance. Experiments with 50% dry basis (V50) showed:

- Higher production velocity: Characteristic times (τ_p) of approximately 30 days, compared to 60 days for V20.
- Improved biogas quality: Methane content above 45%, meeting the threshold to be considered a biofuel (Dueblein and Steinhauser, 2008).
- Greater bioavailability: Higher values of ψ_0 and $\mu_{\max,\,\psi}$ in the Gompertz equation.

Impact of pH control

pH control at 7.5 showed significant effects on production kinetics:

- Increased maximum specific production potential: The Gompertz parameter ψ_0 increased by 15-25% under pH-adjusted conditions, compared to the 125% increase in total cumulative biogas volume observed in V20b vs V20a (Figure 3).
- Change in dynamics: In V20, pH control increased (τ_p) from 60 to 66 days, suggesting a more prolonged microbial adaptation phase, but with greater final biogas production.
- Parameter optimization: Coefficients μ_{eff} and k_p showed consistent increases under pH- adjusted conditions.

It is notable that with V50b (50% substrate, adjusted pH) higher cumulative production values were achieved, confirming the synergy between high substrate concentration and optimal pH conditions.

Implications for biofuel production

The integrated analysis of the obtained parameters allows establishing criteria for biogas production as a biofuel:

- Quality threshold: Only the V50a condition (50% substrate, pH 6.8) approached the 45% biofuel threshold, with a methane content of 41%. While this falls slightly short of the threshold, it demonstrates significant improvement over lower substrate conditions.
- Process efficiency: The combination of high substrate concentration (50%) and pH control increases both kinetics and product quality.
- Scalability: The determined transport coefficients provide a solid basis for designing larger-scale systems.

The consistency among the three models in predicting these behaviors validates the proposed multi-scale approach.

Limitations and practical considerations

Although the models showed predictive capacity, it is important to consider:

- The lag phase (λ_ψ) in the Gompertz equation was negligible in all cases (see comment above for V20a interpretation), possibly due to the use of adapted inoculum.
- The models assume isothermal conditions and complete mixing, which might require adjustments for continuous, larger-scale systems.
- Detailed characterization of tomato waste would be beneficial to establish more correlations.

A comprehensive summary of the results obtained from the mathematical model fitting is presented below.

Table 5. Summary of values and applicability

Parameter	**V20a (20 %, pH 6.8)**	**V20b (20 %, pH 7.5)**	**V50a (50 %, pH 6.8)**	**V50b (50 %, pH 7.5)**
CH_4 (%)	27 %	37 %	41 %	37 %
τ_p (days)	60.2	65.7	30.5	31.2
ψ_0 (L/gVS)	0.245	0.312	0.412	0.523
Qualifies as Biofuel?	No	No	No (approaches threshold at 41%)	No
Operational Recommendation	Not viable	Limited	Optimal for quality	Optimal for productivity

A key limitation of this study is the reliance on aggregated data from Castro-Rivera *et al*. (2020), which did not include detailed characterization of the tomato residue composition (e.g., lignin, cellulose, hemicellulose, and soluble sugar fractions). Variability in these components would directly affect the Michaelis-Menten saturation constant κ_{eff} and effective reaction rate μ_{eff}. For instance, higher lignin content would reduce substrate bioavailability, increase κ_{eff} and decreasing μ_{eff}, while higher soluble sugar content would have the opposite effect. Future work should incorporate detailed substrate characterization and, ideally, conduct sensitivity analyses to quantify how compositional variability propagates through the model parameters.

The consistent near-zero lag phase suggests that future studies on similar substrate-inoculum combinations could employ simpler two-parameter models (e.g., first-order kinetics) without significant loss of predictive power.

Conclusions

This study demonstrates the development and validation of a comprehensive multi-scale modeling approach for biogas production from the anaerobic co-digestion (AcoD) of cattle manure and tomato crop waste. The main conclusions are summarized below:

1. **Robust Multi-Scale Framework**: The cross-validation of the three complementary modeling approaches—Volume Averaging, Laplace Domain, and Modified Gompertz—confirmed their individual predictive accuracy (R^2: 0.84–0.97) and demonstrated their synergistic power. The Volume Averaging model provided the physicochemical foundation for scale-up, the Laplace approach offered tools for dynamic analysis and control, and the Gompertz equation enabled practical kinetic parameterization. This triangulation methodology reduces prediction uncertainty and establishes a robust framework for the design of AcoD systems.
2. **Validated Parameter Determination**: The parameter determination via these models was both effective and consistent with specialized literature. The Volume Averaging model enabled the estimation of fundamental transport coefficients, yielding effective diffusivity values ($\mathcal{D}_A \approx 1.6 \times 10^{-6}$ m^2/d). Crucially, these values align closely with independent experimental data for high solids digestates, specifically with the $\mathcal{D}_A$ range (1.00 to 1.12×10^{-11} m^2/s) reported by Gooddy *et al*. (2007) for total solids contents above 15%. This concordance

validates the proposed modeling tools as reliable methods for estimating transport parameters in complex media. Simultaneously, the Laplace approach provided the system's dynamic parameters $(\tau_p\ ; k_p)$, and the Gompertz equation efficiently quantified the kinetic parameters $(\psi_0; \mu_{\max,\psi})$.

3. **Tools for Process Scale-up**: The integrated methodology provides a practical toolkit for designing larger-scale systems, with specific applications in agricultural regions where tomato waste is an abundant and underutilized byproduct. The determined coefficients $(\mathcal{D}_A, \mu_{\text{eff}}, \kappa_{\text{eff}})$ constitute transferable design parameters for the geometric scaling of reactors. Notably, the inverse relationship between the characteristic time τ_p and substrate concentration (50% vs. 20%) provides a quantitative criterion for optimizing hydraulic retention times in continuous systems. This framework allows for predicting pilot or industrial-scale performance based on laboratory data, reducing the costs and risks associated with empirical scale-up.
4. **Optimized Operational Conditions**: The combination of a high substrate load (50% dry basis) with pH control (7.5) emerged as the optimal condition, maximizing methane yield (4.75 L/gVS) and halving the characteristic production time to approximately 30 days compared to lower-load systems. This condition achieved a methane content above 45%, meeting the threshold for biofuel qualification and directly impacting process profitability by lowering operational costs.
5. **Contribution to Sustainability**: The AcoD of cattle manure and tomato waste presents a viable pathway for decentralized renewable energy generation, contributing to the valorization of agricultural residues and the mitigation of emissions associated with the agro-industrial sector. For the Mexican context, where tomato waste has negligible or negative cost, this approach represents an economically feasible option for enhancing local energy security in farming areas.

Future research should validate this framework in continuous and larger-scale systems, explore its applicability to other regional agricultural wastes, and include systematic sensitivity analyses of critical parameters such as the volume fraction, which was held constant in this study but is expected to significantly influence transport predictions under non-ideal mixing conditions.

In summary, this study sets a methodological precedent for the integrated modeling of AcoD systems, demonstrating that the synergy between fundamental and empirical models can overcome the limitations of isolated approaches. The results validate the AcoD of cattle manure and tomato waste as a technically viable route for biofuel production, achieving the required quality thresholds (>45% CH_4) under optimized conditions. Future research should validate this framework in continuous and larger-scale systems and explore its applicability to other regional agricultural wastes to maximize the impact of bioenergy in the energy transition of developing countries.

Acknowledgments and Funding: The authors wish to express their gratitude for the valuable experimental data provided by the research group led by Castro-Rivera *et al*. (2020), which constituted the experimental basis for the validation of the models. The financial support from Universidad Autónoma Metropolitana for this research is also acknowledged.

Author Contributions: G.B.-O.: Conceptualization, Methodology, Formal analysis, Software, Validation, Writing – original draft, Writing – review & editing; A.T.-A.: Methodology, Data curation, Formal analysis, Software, Validation, Writing – review & editing; R.L.-L.: Conceptualization, Supervision, Project administration, Funding acquisition, Writing – review & editing; H.D.L.-M.: Conceptualization, Methodology, Formal analysis, Validation, Supervision, Project administration, Funding acquisition, Writing – original draft, Writing – review & editing; V.C.H.-F.: Methodology, Data curation, Formal analysis, Validation, Writing – review & editing.

References

Alburquerque, J. A., de la Fuente, C., Ferrer-Costa, A., Carrasco, L., Cegarra, J., Abad, M., & Bernal, M. P. (2012). Assessment of the fertiliser potential of digestates from farm and agroindustrial residues. *Biomass and Bioenergy, 40*, 181–189. https://doi.org/10.1016/j.biombioe.2012.02.018

Alghoul, O., El-Hassan, Z., Ramadan, M., & Olabi, A. G. (2019). Experimental investigation on the production of biogas from waste food. *Energy Sources, Part A: Recovery, Utilization, and Environmental Effects, 41*(19), 2051–2060. https://doi.org/10.1080/15567036.2018.1549156

Benítez-Olivares, G., Valdés-Parada, F. J., & Saucedo-Castañeda, J. G. (2016). Derivation of an upscaled model for mass transfer and reaction for non-food starch conversion to bioethanol. *International Journal of Chemical Reactor Engineering, 14*(4), 1115–1148. https://doi.org/10.1515/ijcre-2016-0004

Bird, R. B., Stewart, W. E., & Lightfoot, E. N. (2002). *Transport phenomena* (2nd ed.). Wiley.

Börjesson, P., & Mattiasson, B. (2008). Biogas as a resource-efficient vehicle fuel. *Trends in Biotechnology, 26*(1), 7–13. https://doi.org/10.1016/j.tibtech.2007.09.007

Castro-Rivera, R., Solís-Oba, M., Chicatto-Gasperín, V., & Solís-Oba, A. (2020). Producción de biogás mediante codigestión de estiércol bovino y residuos de cosecha de tomate (*Solanum lycopersicum* L.). *Revista Internacional de Contaminación Ambiental, 36*(3), 529–539. https://doi.org/10.20937/rica.53545

Chaemchuen, S., Zhou, K., & Verpoort, F. (2016). From biogas to biofuel: Materials used for biogas cleaning to biomethane. *ChemBioEng Reviews, 3*(5), 250–265. https://doi.org/10.1002/cben.201600016

Düblein, D., & Steinhauser, A. (2008). *Biogas from waste and renewable resources*. Wiley-VCH.

Elagroudy, S., Radwan, A., Banadda, N., Mostafa, N., Owusu, P., & Janajreh, I. (2020). Mathematical models comparison of biogas production from anaerobic digestion of microwave pretreated mixed sludge. *Renewable Energy, 155*, 1009–1020. https://doi.org/10.1016/j.renene.2020.03.166

Esposito, G., Frunzo, L., Giordano, A., Liotta, F., Panico, A., & Pirozzi, F. (2012). Anaerobic co-digestion of organic wastes. *Reviews in Environmental Science and Bio/Technology, 11*, 325–341. https://doi.org/10.1007/s11157-012-9277-8

González-Herrera, E., Hernández-Beltrán, J., López-González, Y., Mailín, L., & Jiménez-Hernández, J. (2021). Digestión anaerobia de suero de queso utilizando inóculo de estiércol porcino a diferentes relaciones inóculo-sustrato. *Centro Azúcar, 48*(3), 11–20.

Gooddy, D., Kinniburgh, D., & Barker, J. (2007). A rapid method for determining the diffusion coefficient in digestion medium using a diffusion cell. *Journal of Hydrology, 343*(1–2), 97–103. https://doi.org/10.1016/j.jhydrol.2007.06.014

Hatata, A., Galal, O., Said, N., & Ahmed, D. (2021). Prediction of biogas production from anaerobic co-digestion of waste activated sludge and wheat straw using two-dimensional mathematical models and an artificial neural network. *Renewable Energy, 178*, 226–240. https://doi.org/10.1016/j.renene.2021.06.050

Hernandez-Fydrych, V., Benítez-Olivares, G., Fajardo-Ortiz, M., Rojas-Zamora, U., & Salazar-Pelaez, M. (2021). Analysis of the transient inhibited steady state in anaerobic digestion of a semisolid from pretreated slaughterhouse wastewater. *Revista Mexicana de Ingeniería Química, 20*(2), 541–553. https://doi.org/10.24275/rmiq/IA2012

Hernández-Fydrych, V., Benítez-Olivares, G., Meraz-Rodríguez, M., Salazar-Pelaez, M., & Fajardo-Ortiz, M. (2019). Methane production kinetics of pretreated slaughterhouse wastewater. *Biomass and Bioenergy, 130*, 105385. https://doi.org/10.1016/j.biombioe.2019.105385

Hilaire, F., Basset, E., Bayard, R., Gallardo, M., Thiebaut, D., & Vial, J. (2017). Comprehensive two-dimensional gas chromatography for biogas and biomethane analysis. *Journal of Chromatography A, 1524*, 222–232. https://doi.org/10.1016/j.chroma.2017.09.071

Khadka, A., Parajuli, A., Dangol, S., Thapa, B., Sapkota, L., Carmona-Martínez, A. A., & Ghimire, A. (2022). Effect of the substrate to inoculum ratios on the kinetics of biogas production during the mesophilic anaerobic digestion of food waste. *Energies, 15*(3), 834. https://doi.org/10.3390/en15030834

Kumar, A., & Samadder, S. R. (2020). Performance evaluation of anaerobic digestion technology for energy recovery from organic fraction of municipal solid waste: A review. *Energy, 197*, 117253. https://doi.org/10.1016/j.energy.2020.117253

Levenspiel, O. (1998). *Chemical reaction engineering* (3rd ed.). Wiley.

Li, Y., Chen, Z., Peng, Y., Huang, W., Liu, J., Mironov, V., & Zhang, S. (2022). Deeper insights into the effects of substrate-to-inoculum ratio selection on kinetic parameters and microbial communities during anaerobic digestion of food waste. *Water Research, 217*, 118440. https://doi.org/10.1016/j.watres.2022.118440

Mendivil-Garcia, K., Amabilis-Sosa, L., Rodríguez-Mata, A., Rangel-Peraza, J., Gonzalez-Huitron, V., & Cedillo-Herrera, C. (2020). Assessment of intensive agriculture on water quality in the Culiacán river basin, Sinaloa, México. *Environmental Science and Pollution Research, 27*, 28636–28648. https://doi.org/10.1007/s11356-020-08653-z

Monod, J. (1949). The growth of bacterial cultures. *Annual Review of Microbiology, 3*, 371–394. https://doi.org/10.1146/annurev.mi.03.100149.002103

Nock, W. J., Walker, M., Kapoor, R., & Heaven, S. (2014). Modeling the water scrubbing process and energy requirements for CO_2 capture to upgrade biogas to biomethane. *Industrial & Engineering Chemistry Research, 53*(31), 12783–12792. https://doi.org/10.1021/ie501280p

Ochoa, J., Stroeve, P., & Whitaker, S. (1986). Diffusion and reaction in cellular media. *Chemical Engineering Science, 41*(11), 2999–3013. https://doi.org/10.1016/0009-2509(86)85036-9

Picioreanu, C., van Loosdrecht, M. C. M., & Heijnen, J. J. (1998). Mathematical modeling of biofilm structure with a hybrid differential-discrete cellular automaton approach. *Biotechnology and Bioengineering, 58*(1), 101–116. https://doi.org/10.1002/(SICI)1097-0290(19980405)58:1<101::AID-BIT11>3.0.CO;2-M

Ravina, M., Castellana, C., Panepinto, D., & Zanetti, M. (2019). McBioCH_4: A computational model for biogas and biomethane evaluation. *Journal of Cleaner Production, 227*, 739–747. https://doi.org/10.1016/j.jclepro.2019.04.224

Secretaría de Energía. (2020). *Programa Sectorial de Energía 2020–2024*. Diario Oficial de la Federación. https://www.dof.gob.mx

Servicio de Información Agroalimentaria y Pesquera. (2023). *Expectativas agroalimentarias*. https://www.gob.mx/siap

Velázquez-Martí, B., Meneses-Quelal, O. W., Gaibor-Chavez, J., & Niño-Ruiz, Z. (2018). Review of mathematical models for the anaerobic digestion process. In *Anaerobic digestion*. IntechOpen. https://doi.org/10.5772/intechopen.80815

Whitaker, S. (1999). *The method of volume averaging*. Kluwer Academic Publishers.

Widder, D. V. (2015). *Laplace transform* (PMS-6). Princeton University Press.

Zwietering, M. H., Jongenburger, I., Rombouts, F. M., & Van't Riet, K. (1990). Modeling of the bacterial growth curve. *Applied and Environmental Microbiology, 56*(6), 1875–1881. https://doi.org/10.1128/aem.56.6.1875-1881.1990

A Web Platform for Virtual Interpretive Water Trails

Sonia González-Márquez [1], Eric Houbron [2], Emanuel Lucho-Xala [1] and Gloria Inés González-López [2,*]

[1] Facultad de Informática, Universidad Veracruzana, Veracruz, Veracruz, Mexico
[2] Facultad de Ciencias Químicas, Universidad Veracruzana, Orizaba, Veracruz, Mexico
* Corresponding author glorgonzalez@uv.mx; Tel.: ((52) 2291106408)

Received: August 20, 2025 Accepted: October 2, 2025 Published: June 1, 2026
DOI: https://doi.org/10.56845/rebs.v8i2.663

Abstract: The Universidad Veracruzana (UV), through its Sustainability Coordination (Cosustenta), promotes awareness about environment protection and water resources by means of interpretive trails. To support this activity, a research group developed a software platform to manage all the digital resources needed to offer this educational online tool. The goal is to extend environmental education to people who for several reasons cannot participate in an in-situ visit. As a first step, the material of several environmental organizations that offer online educational resources was reviewed in order to analyze the interfaces, services and resources that they provide, including images, videos, audio files, among others. SCRUM was selected as the agile software development methodology, and open-source software such as PostgreSQL, XAMPP, PHP, HTML, CSS, GitHub, Bootstrap, was used. A relational database was designed to manage data from a web server with internet access. This database can host multiple interpretive trails with specific data and multimedia resources. The software uses educational material designed by Cosustenta for the Health Sciences Unit in Xalapa, Veracruz to show how it works; it also uses resources in several formats to enrich the user experience at each stop along the trail. The result is a web application called SENDINA, which promotes environmental education by integrating technology with sustainability.

Keywords: environmental education, interpretative trails, multimedia platform, sustainability

Introduction

Climate change, biodiversity loss, and environmental pollution represent urgent challenges for the planet and humanity, which are addressed by Environmental Engineering through the planning and execution of technical projects as well of the design of educational strategies to generate changes in people's perception and behavior. In this context, educational trails constitute valuable scenarios for developing environmental awareness among the population and an excellent tool, based on socio-environmental communication, to promote sustainable behavior models (Environmental Education Lanzarote, 2025).

An interpretive trail (also known as an educational, pedagogical, or instructional trail) is a planned route within a natural or semi-natural space that includes informational or interactive stations. These stations address environmental, scientific, cultural, or technical topics and allow visitors to observe, reflect, and learn while walking through the area. Its main objective is to educate visitors about the value of natural resources, local environmental problems, and possible solutions, many of which are directly related to Environmental Engineering (Rumbonaturaleza, 2022).

Environmental Engineering focuses on developing technical solutions for problems such as water management, waste treatment, and remediation of contaminated soils. However, educational support must also be developed to promote public participation. Environmental education should not be limited to classroom instruction or passive information campaigns; it needs to engage people emotionally and cognitively so they can directly experience and understand the importance of the natural environment. Educational trails fulfill this function by offering a learning experience through direct contact with ecosystems (Knowledge Hub, 2023).

Educational institutions play a crucial role in building more just, equitable, and sustainable societies through their teaching, research, and outreach functions. Universities, specifically, train future professionals who will participate in the political, social, and economic life of society. Universidad Veracruzana recognizes this and has been committed since 2010 to developing institutional policies that incorporate a sustainability perspective into teaching, research, outreach, and management functions. This commitment is demonstrated through the University Coordination for Sustainability (Cosustenta UV) (Cosustenta, 2025), which has implemented interpretive water trails accessible to both members of its academic community and the public, to awareness about the importance of water resource conservation.

This paper presents a proposal for a web application that offers the opportunity to explore water-related interpretive trails to the public, who for several reasons cannot physically visit them. This tool expands access to environmental education and raises awareness within society. An online platform allows users to enjoy a virtual experience where they can explore, learn, and understand the importance of natural resource conservation from any internet-connected device at any time, without the need to physically visit the location.

SENDINA (Interpretive Trails of Water) is a web application that provides a preliminary overview of the Interpretive Trail of Water at Health Sciences Unit of Universidad Veracruzana in the city of Xalapa. It contains relevant information for each station along the trail, displaying photographs, videos, and other multimedia materials through virtual panels (Lucho, 2024).

SENDINA allows the creation of interpretative trails with their respective stations and multimedia materials, not only for the Xalapa Region but for any of the five zones of the Universidad Veracruzana, for which the system was originally designed. The software application has a flexible structure, and can manage multiple trails, each with several stations, each containing different types of educational material (Lucho, 2024).

Materials and Methods

This section describes the methodological framework used to analyze existing interpretative trails and to design and implement the proposed web platform.

Virtual Trails

Interpretive trails are present around the world and have increased in number due to the growing interest of organizations in environmental sustainability. However, during the Covid-19 pandemic many interpretive trails were temporally closed to protect public health, which boosted the development and implementation of online tools. These platforms give people the ability to interact with and learn from trails without leaving home, by incorporating digital visualization and multimedia resources to offer users interactive learning experiences without the need for physical travel (Lucho, 2024).

Some examples of interpretive trails that embraced digital transformation and became not only physical but also virtual experiences are presented.

Red Front Trail

This is a remarkable example of natural resource management focused on ecosystem conservation and habitat protection. It also hosts the Yale School of the Environment, dedicated to postgraduate training in forestry management. The trail is in Montana, United States, with a 1.5 km route that runs through a section of extensive Yale-Myers forest (Figure 1). The path comprises 14 stations that address themes related to forest health, wildlife habitat conservation and native species diversity (Yale Forests, 2024a).

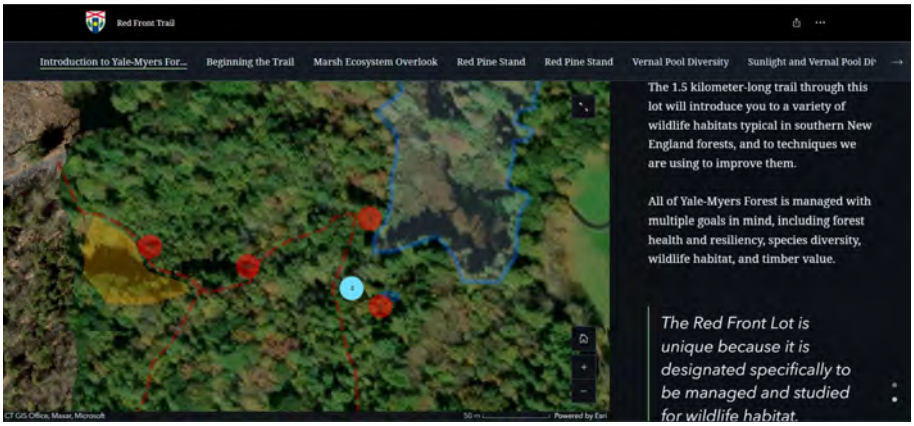

Figura 1. Módulo fotovoltaico de 40 celdas conformado por 4 strings

On May 4, 2020, the Office of School Forests launched an online platform called “Story Map," which allows users to virtually explore the trail. This platform is full of photos and descriptions of wildlife habitat along the trail, which reflects

countless contributions to trail construction, writing, research, and design over the years from staff, students, and faculty (Yale Forests, 2024b).

Newcomb Naturalis

The College of Environmental Science and Forestry of State University of New York State have several interpretive trails where thousands of visitors and local residents participate in educational programs within Adirondack Park, an unique natural, cultural, and recreational resource in New York. These trails include the R.W. Sage Jr. Memorial Trail, Rich Lake Trail, Peninsula Trail, and Sucker Brook Trail. They address several topics related to coniferous forests, Rich Lake, and the ecosystems of this region (State University of New York College of Environmental Science and Forestry [ESF], 2024).

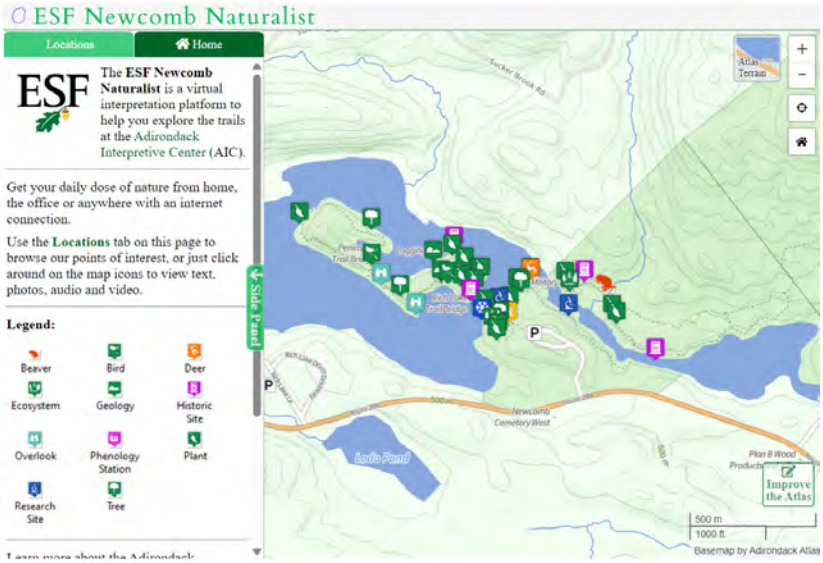

Figure 2. Newcomb Naturalis Map

Despite the simplicity of the platform (Figure 2), it displays all points of interest along each trail and provides brief information about each station.

Rain Garden interpretative Trail

This trail is located in the suburbs of the Rain Garden in West Torrens, South Australia. The trail map (Figure 3) shows stations focused on rainwater harvesting and collection from rooftops, roads, and paths. It contains ten stations, and therefore the trail can be explored on foot or by bicycle (Westtorrens, 2023).

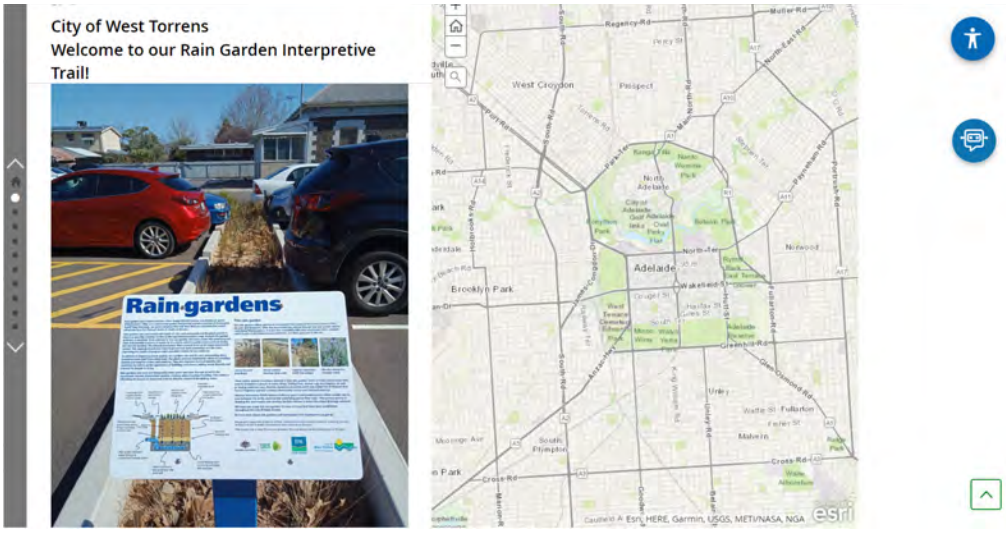

Figure 3. Rain Garden interpretive trail

In Mexico, there are several interpretive trails focused on sustainability and environmental awareness; however, few of them have digital platforms that allow virtual exploration . This represents a significant opportunity for people unable to travel and visit these trails personally. Therefore, it is important to highlight the relevance of virtual format for Universidad Veracruzana interpretive water trails, because as it can broaden acces and facilitate environmental education for a larger audience.

Universidad Veracruzana Trails

In 2018, the University Center for Arts, Sciences, and Culture, Córdoba (CUACC), became the first center with an interpretive trail called “Saturday with Nature.” This trail allows people to learn about several topics and to participate in many outdoor activities focused on sustainable living. Some of topics covered on this trail are: 1) Carbon Cycle; 2) Water Cycle; 3) Archaeological History; and 4) A garden of medicinal, culinary, and aromatic plants (Universidad Veracruzana [UV], 2024).

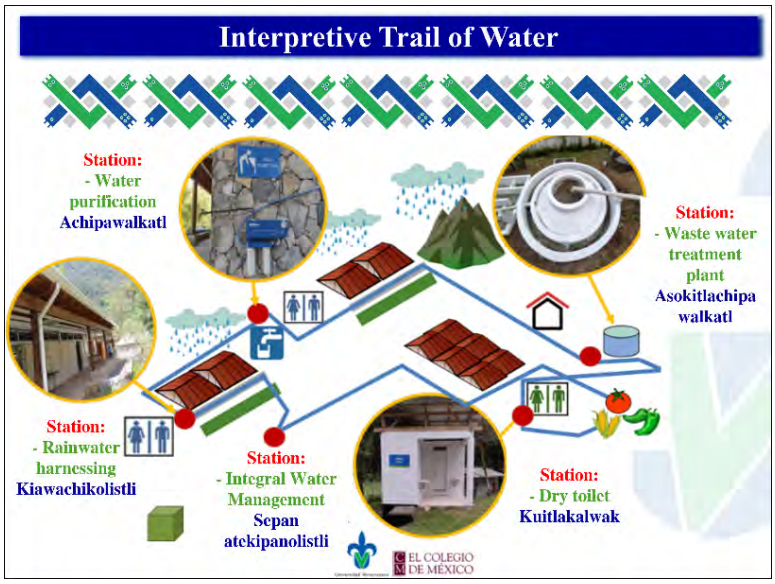

Figure 4. SIA stations

In 2022, a second trail was implemented, with a Nahuatl name “Tehwan ti ameh” (Figure 4), or “Interpretive Trail of Water (SIA)”. Students from Environmental Engineering, Architecture, and Intercultural Management for Development, careers at Universidad Veracruzana (UV) in Orizaba-Córdoba region and El Colegio de México participated in this development (UV, 2023). This trail was based at the Universidad Veracruzana Intercultural (UVI), Grandes Montañas campus, with a purpose: to address, with local communities in Zongolica region, the significant challenge to water access and its comprehensive and sustainable management (Figure 4).

The trail consists of eight educational stations within the UVI facilities, accessible through a 90-minute guided tour offered in both Spanish and Nahuatl. This stations invite visitors to reflect on: 1) The relationship between humans, water, and climate change; 2) rainwater harnessing, 3) water purification, 4) wastewater management, 5) a wastewater treatment plant, 6) wetlands; 7) dry toilet and 8) composting (UV, 2024).

In 2023, in the “Cells for Sustainability” project, Interpretive Trail of Water was created for Health Sciences Unit–Xalapa (UCS-X) with the purpose of creating awareness in university community and society about sustainability issues related to the integrated management of water resources (Figure 5). This project is directed to university community: students, teachers, administrative staff, and users of medical services offered by UCS-X. The Interpretive Trail of Water represents an educational opportunity specifically about relationship between water and users as well as influence on health. According to the type of UCS-X visitors, the trail can be visited with a guide or by themselves. The UCS-X Interpretive Trail of Water contains eight educational stations: 1) Map of Interpretive Trail of Water at UCS-X; 2) People, Water, and Health; 3) Water and Green Areas; 4) Rainwater harnessing and storage; 5) Water treatment; 6) Waste water; 7) Water and energy, and finally 8) Water and science (UV, 2024).

Figure 5. UCS-X Trail Launching

Scrum

Scrum is a framework for agile software development thath has been extended to other areas, as it provides a set of best practices for collaborative teams to achieve optimal results in project development (Agile Projects, n.d.). This methodology helps organize teams, enabling them to learn from experience and adapt to change; it is particularly useful in software development for solving complex problems in an efficient and sustainably manner (Amazon Web Services [AWS], 2024). It consists of different stages, as illustrated in Figure 6 (Synapptica, 2025).

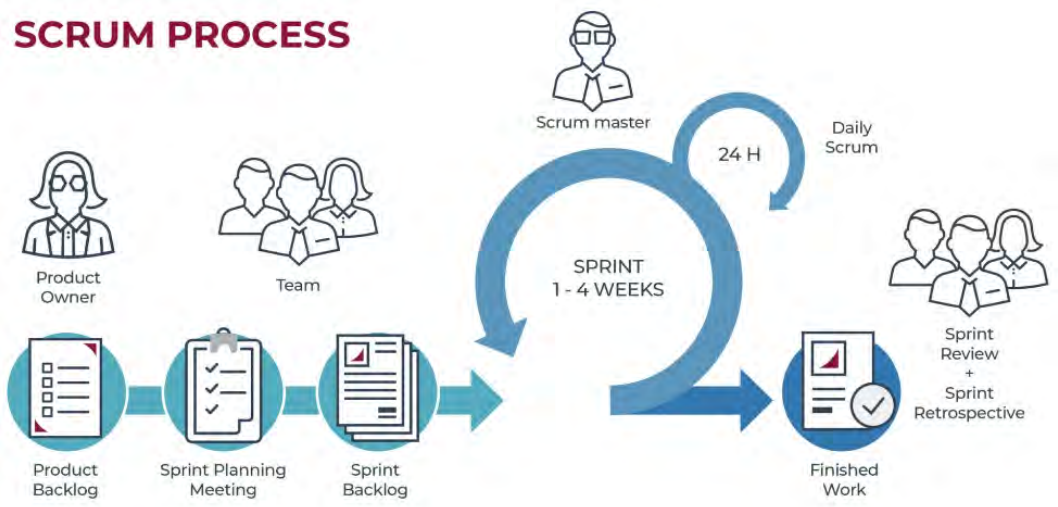

Figure 6. SCRUM model stages

Development Software

Figure 7 presents the software tools used to develop the web application, along whit a brief description of each component.

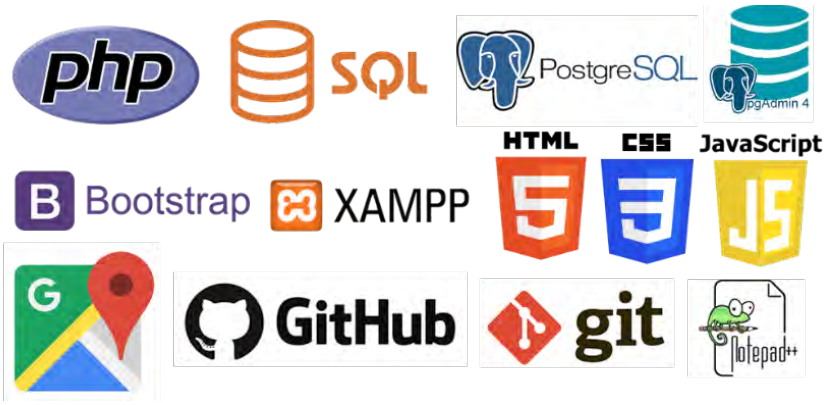

Figure 7. Software tools used in web application development

A relational database model was implemented using PostgreSQL version 15.2,selected for its robustness and ease of use. For database design, administration, and querying, pgAdmin4 was selected. This integrated tool provides a graphical interface for database management and it is used along with XAMPP, a free and open-source platform for local web application development,enabling both database management and web server operation. Notepad++, a text editor supporting multiple programming languages and plugin integration was also used (Lucho, 2024). The backend was developed using PHP (Hypertext Preprocessor), an open-source scripting language designed for dynamic web applications; where code execution occurs on the server prior to being sent to the client's browser. For the frontend, Bootstrap, a free and open-source framework, was used in combination with HTML (HyperText Markup Language) and CSS (Cascading Style Sheets), to define the visual appearance of web interface, including layout, colors, and typography (Lucho, 2024). The Google Maps API (Application Programming Interface) was integrated to display the geographical location of each station along the trail, while JavaScript was used to implement interactive elements and animations (Google, 2025).

The project was developed using GitHub, an online platform for version control and collaborative software development. Git, an open-source version control system, was used to manage code changes and facilitate collaboration among multiple users (Lucho, 2024).

According to Scrum methodology, the Product Backlog defines priority tasks and development stages,including: Requirements Analysis, Database Design, Backend Development, and Frontend Development. At each stage, user stories are definide to specifytasks, timelines, and progress tracking.

Once user requirements are identified and documented, the database design process begins (Figure 8). This includes the development of a relational model, data dictionary, and system implementation. Tables, relationships, views, and queries are designed, as well as reports requested through the interface. Finally, user interfaces to facilitate web browsing are developed, defining color palette, font styles, component layout, and logos and images to be displayed.

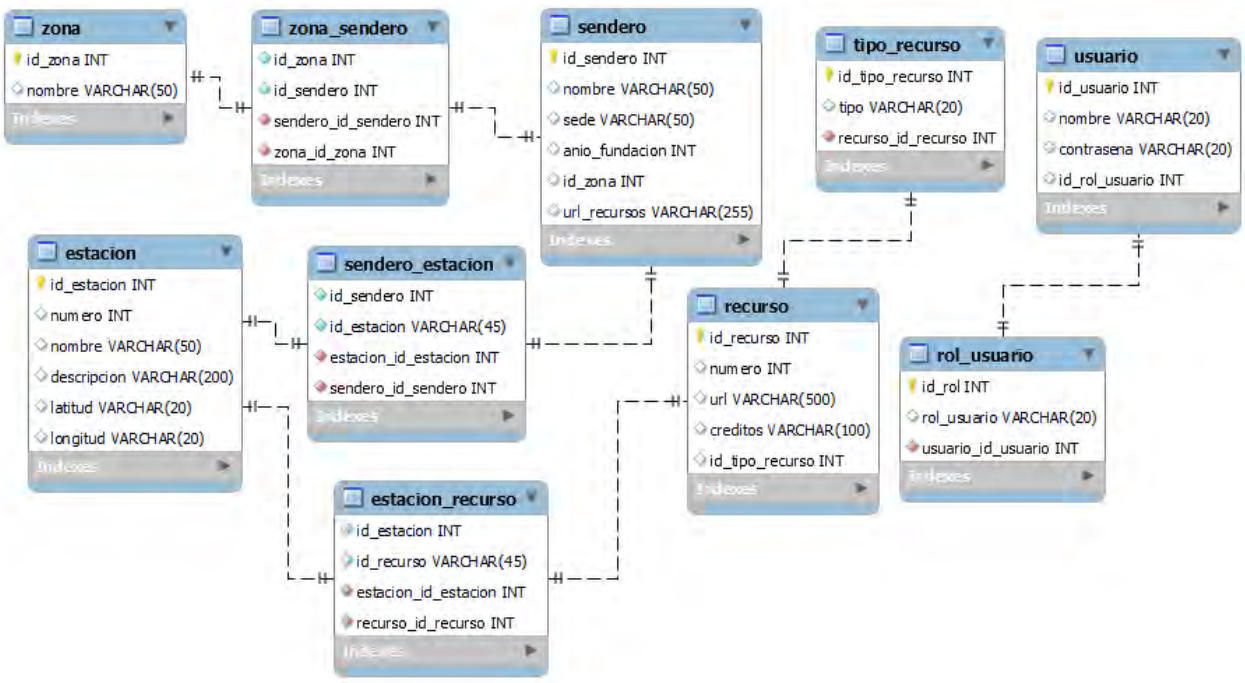

Figure 8. Relational database model

The main interface of the web application is shown in Figure 9.

Figure 9. Section of the Sendina home page

Data from the interpretive Trail of Water at the Xalapa Health Sciences Unit (UCS-X) i were used to demonstrate the functionality of the platform (Figure 10).

Researchers from the Environmental Engineering area at Cosustenta defined the components to be included, ensuring that each station displays multimedia material according to its content. Figure 11 shows the complete trail map, where users can navigate through two panels: the left panel displays multimedia content for each station, while the right panel shows the current location on the trail. A location icon indicates each station along the route, and when the cursor is placedover the symbol, the available multimedia resources are displayed.

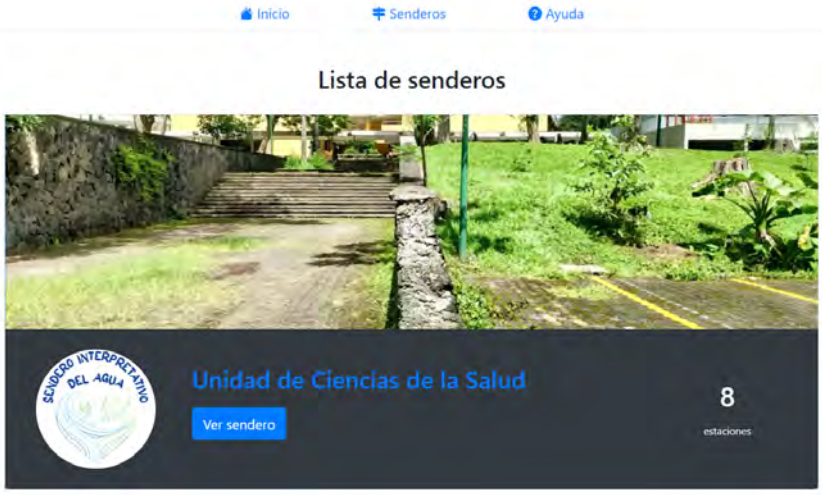

Figure 10. UCS-X interpretive trail

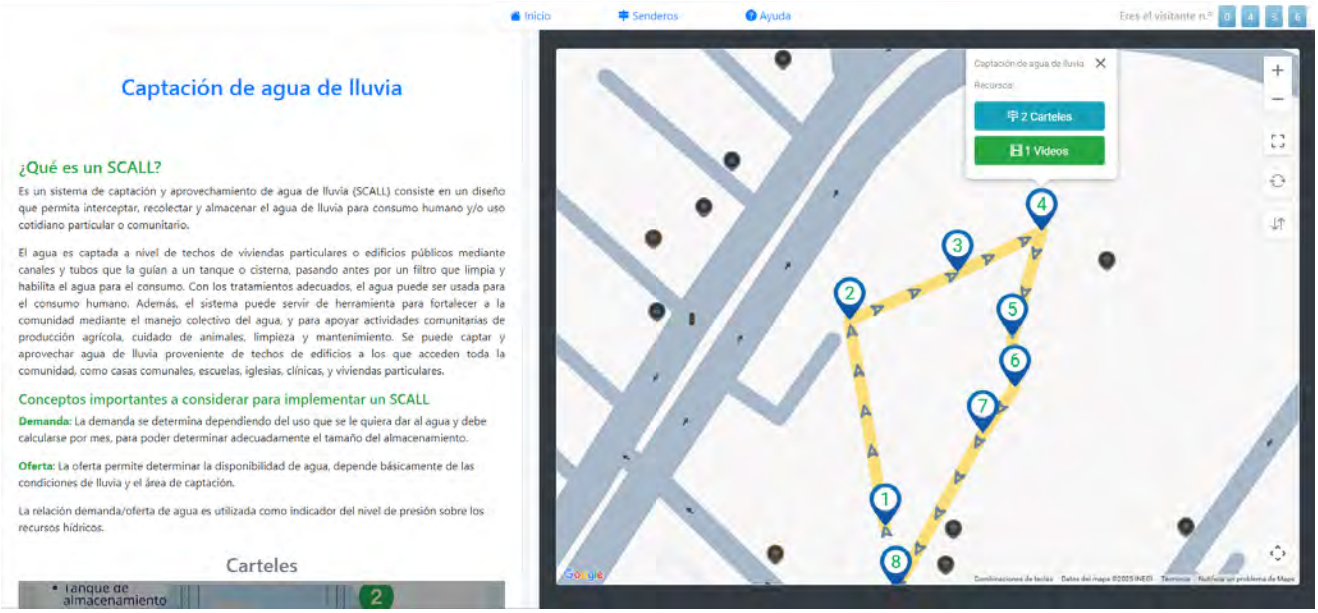

Figure 11: Section of UCS-X interpretive trail map

End users cannot modify the application or its data and are limited to browsing functionalities. The creation of new trails, including their stations and associated content, is restricted to authorized users through a dedicated management interface Only authorized and registered users are permitted to modify the platform content.

Results and Discussion

A free web application called Sendina was created and is hosted at the following URL: http://iiuv.org/Sendina/. It offers a responsive design that allows users to access and navigate its content from any electronic device with internet access. Its main objective is to manage interpretive trails created by the UV Cosustenta program, ensuring that environmental education reaches the largest audience. The platform is specifically focused on trails related to water resource conservation and initially displays the content of UCS-X Interpretive Trail of Water. This trail has eight stations located throughout the unit area, which are shown on a Google map that can be explored using the application functions, including zoom in and out, map panning, map rotation, and full-screen mode.

If users have a slow internet connection, they may experience slow loading times when displaying images on the website due to the size and quality of the multimedia resources offered. Sendina allows the inclusion of additional trails; however, the geographic coordinates of the stations and their corresponding multimedia material are required. There is no predefined limit to the number of trails that can be incorporated, nor the number of stations within each trail. As a suggestion for future improvements, additional resources that enrich the virtual experience, such as panoramic images, 360° views, or interactive environments, could be incorporated into the platform.

Conclusions

Interpretive trails, from an Environmental Engineering perspective, represent a strategic tool for promoting environmental awareness in society. These spaces allow people to connect technical knowledge with real experience, to thereby facilitating the understanding of environmental challenges and motivate the population to take care of natural resources. The integration of interpretive trails into sustainable development initiatives is fundamental for moving towards a more informed, participatory, and environmentally conscious society.

The future of the planet largely depends on collective decisions; therefore, experiential environmental education represents and effective approach to fostering responsible environmental behavior.

Among the main benefits of interpretive trails are the promotion of critical thinking, active and meaningful learning, behavioral changes towards environmental protection, and the stimulation of ecotourism and local development. The “Tehuan ti ameh” trail represents a relevant example of this educational and environmental benefits within the context of the Universidad Veracruzana initiatives.

Acknowledgments and Funding: We appreciate all the support that Universidad Veracruzana Cosustenta has provided for this project.

Author contributions: G.M.-S.: Data analysis and database design; H.-E.: Data collection, multimedia material design; L. X.-E.: Sofware design and coding; G. L.-G.: Writing and supervision.

References

Amazon Web Services. (2024). *¿En qué consiste Scrum?* https://aws.amazon.com/es/what-is/scrum/
Cosustenta. (2025). *Bienvenida*. https://www.uv.mx/cosustenta/bienvenida/
Educación Ambiental Lanzarote. (2025). *Senderos educativos*. https://educacionambientallanzarote.com/senderos-educativos/
García, L. R. (2019). *Guía para el diseño y operación de senderos interpretativos*. https://www.sib.gob.ar/portal/wp-content/uploads/2019/02/Gu%C3%ADa-para-el-Dise%C3%B1o-y-Operaci%C3%B3n-de-Senderos-Interpretativos.pdf
Google. (2025). *Google Maps platform*. https://developers.google.com/maps/documentation/javascript/overview?hl=es-419
Lucho X., E. (2024). *Plataforma web para el sendero interpretativo del agua* [Bachelor thesis]. Universidad Veracruzana. https://uvmx-my.sharepoint.com/:f:/g/personal/abzamora_uv_mx/EkZWbYlyMpJKu1rC9Gu1brUBTCkp7XhRBIMrYQdm_9-nAw?e=N3k5Ec
Polo del Conocimiento. (2023). Sendero pedagógico: una nueva estrategia educativa en el proceso de enseñanza aprendizaje. *8*(9), 1782–1794. https://polodelconocimiento.com/ojs/index.php/es/article/download/6157/15543
Proyectos agiles. (s. f.). *Proyectos agiles. Que es Scrum*. https://proyectosagiles.org/que-es-scrum/
Rumbonaturaleza. (2022). *Senderismo interpretativo: qué es, sus beneficios, características, cómo hacer un sendero interpretativo y más*. https://rumbonaturaleza.com/blog/senderismo/senderismo-interpretativo/
State University of New York College of Environmental Science and Forestry. (2024). *Trail map*. https://www.esf.edu/aic/trails.php
Synapptica. (2025). *Dar los primeros pasos en Scrum*. https://synapptica.net/metodologia-scrum.html
Universidad Veracruzana. (2023). *Sendero interpretativo del agua “Tehwan ti ameh”*. https://www.uv.mx/sustentable/files/2023/08/Sedero_del-agua_Bis_compressed.pdf
Universidad Veracruzana. (2024). *Sendero interpretativo del agua UCS Xalapa – UV Sustentable*. https://www.uv.mx/sustentable/senderointerpretativoucsxalapa/
West Torrens. (2023). *City of West Torrens: rain garden interpretive trail*. https://www.westtorrens.sa.gov.au/Environment-and-Sustainability/Water/Rain-garden-interpretive-trail
Yale Forests. (2024a). *Red front trail*. *ArcGIS StoryMaps*. https://storymaps.arcgis.com/stories/0a01ba29c0874fa480f7b6ef8712ebd7
Yale Forests. (2024b). *Introducing the Red Front Trail StoryMap!* https://forests.yale.edu/news/introducing-red-front-trail-storymap